Swedish University of Agricultural Sciences
Department of Aquatic Science and Assessment

Temporal trends in mercury, methylated mercury and their relation to dissolved organic carbon: Simulation with the Riparian Integration Flow-Concentration Model

Jason A. GALLOWAY
2015

Swedish University of Agricultural Sciences
Department of Aquatic Science and Assessment

Temporal trends in mercury, methylated mercury and their relation to dissolved organic carbon: Simulation with the Riparian Integration Flow-Concentration Model

Jason Austin Galloway

Course code:	EX0431
Course name:	Independent Project in Environmental Science - Master's thesis
Credits:	30.0 ETCS
Supervisor:	Prof. Dr. Kevin Bishop Section for Geochemistry and Hydrology Institutionen för vatten och miljö Lennart Hjelms väg 9 Uppsala
Co-supervisor:	Priv.-Doz. Dr. Markus Puschenreiter Institute of Soil Research Konrad Lorenz-Straße 24 3430 Tulln an der Donau
Examiner:	Prof. Dr. Martyn Futter Section for Geochemistry and Hydrology Lennart Hjelms väg 9 Uppsala
Place of publishing:	Uppsala, Sweden
Level:	E
Program:	Environmental Science in Europe (EnvEuro)
Year of publication:	2015
Picture cover:	Vindel River in Sweden (Photo: Jason Galloway)
Online publication:	http://stud.epsilon.slu.se
Key words:	Mercury, RIM, Riparian Integration Flow-Concentration Model

Acknowledgements

I would like to thank Kevin, Mattias and Markus, for all of their support, comments, direction in developing my thesis. I am also grateful to Staffan, whose lecture on mercury in Sweden piqued my initial interest in getting involved in mercury research in Sweden. I would also like to extend my gratitude to my examiner Martyn for his constructive comments and feedback. Finally I would like to thank all of the colleagues involved in the Krycklan Catchment study for providing such great datasets to work with!

Contents

Index and Abbreviations

Abbreviations

DOC	Dissolved organic carbon
Hg	Mercury
MAE	Mean absolute error
MeAE	Median absolute error
MeHg	Methylated mercury
MK	Mann-Kendall trend test
NSE	Nash-Sutcliffe coefficient
Hg_{tot}	Total mercury
RIM_{dyn}	Dynamic Riparian Flow-Concentration Integration Model
RIM_{med}	Dynamic-Median Riparian Flow-Concentration Integration Model
RIM_{static}	Static Riparian Flow-Concentration Integration Model
RMSE	Root mean squared error

List of Figures

List of Tables

Abstract

Mercury (Hg) and methylated mercury (MeHg) are major environmental pollutants in boreal regions. Dissolved organic carbon (DOC) has been established by a number of studies to be a key vector in the mobilisation of terrestrial Hg and MeHg to aquatic environments where Hg and MeHg can then enter the food chain.

This study examined long-term trends in DOC (1986-2012), Hg (1993-2000) and MeHg (1993-2000) stream water concentrations in three sites (C2- forest, C4- mire and C7 - mixed) in the Svartberget catchment in northern Sweden. A positive trend was found in DOC concentrations over the last decade while results for Hg and MeHg were inconclusive.

The Riparian Flow-Concentration Integration Model (RIM) in three forms (RIM_{static}, RIM_{dyn} and RIM_{med}) was then used to simulate stream water concentrations using flow as an input and model residuals were examined to provide insight into solute dynamics in the three study sites through time. Model residuals were compared and the Nash-Sutcliffe model efficiency coefficient was used to assess the performance of each model at each site.

1. Introduction

1.1 The basic properties of Mercury

Mercury (Hg) is a naturally occurring metallic element; its chemical properties have led to it being used in a number of medicinal, industrial and scientific applications. A summary of the main properties of Hg can be seen in table 1.1. As Hg is a constituent element of the Earth, its production and mobilisation occurs as a natural part of the Earth's biogeochemical cycle through processes such as volcanic eruption and evasion from plants, soils and water bodies (Selin 2009; United Nations Environmental Programme, Chemicals 2002). However, natural background concentrations of Hg have been significantly augmented (30% - 70% depending on continent (Travnikov 2005) due to anthropogenic activities such as coal combustion, mining and other industrial processes (Selin 2009).

Property	Value
Chemical symbol	Hg
Atomic number	80
Density	$13.534\,\mathrm{g\,cm^{-3}}$
Melting point	$-38.8290\,^{\circ}\mathrm{C}$
Atomic mass	$200.592 \pm 0.003\,\mathrm{u}$

Table 1.1: Basic overview of the chemical properties of mercury.

1.2 Mercury in the environment

Hg's relatively high vapour pressure and low water solubility has allowed for its long-range transportation and subsequent accumulation in soils and sediments (Schroeder, Munthe, and Lindqvist 1989). Hg from anthropogenic sources is generally emitted into the atmosphere as elemental mercury [Hg(0)], divalent mercury [Hg(II)] or mercury associated with particulate matter [Hg(p)] (Selin 2009). These emissions can be transported long distances until it is deposited into lakes and soils via precipitation or plant processes. A conceptual model can be seen in figure 1.1.

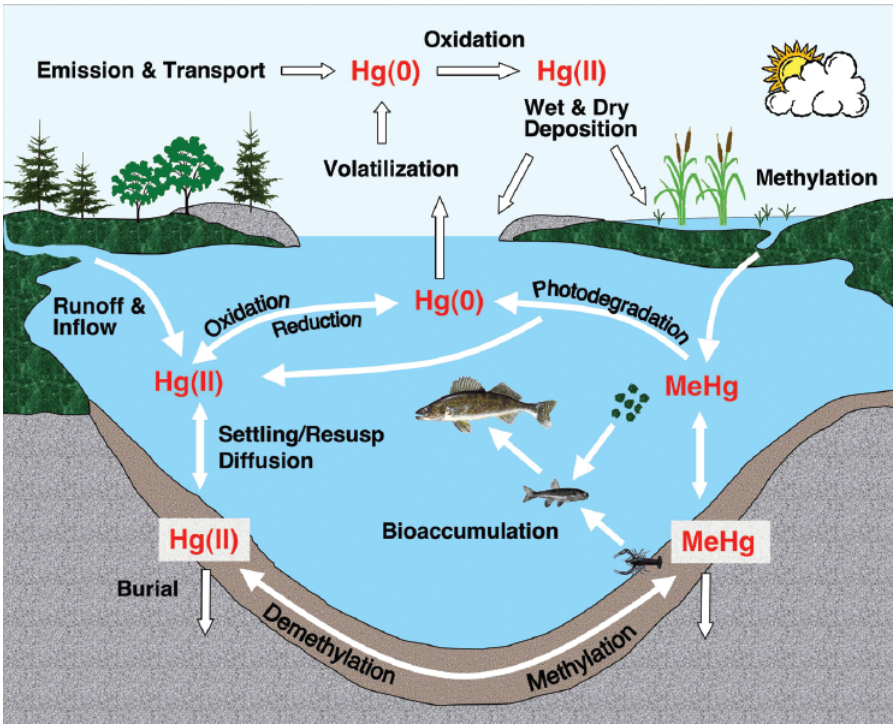

Figure 1.1: Conceptual model showing the movement and speciation of mercury throughout the environment. Engstrom in Selin 2009.

1.3 Mercury speciation and toxicity

Hg exists in the environment in many different chemical forms and as part of a number of complexes, the specific speciation and the compound to which (if any) Hg is bound will determine its mobility and eco-toxicity (Gochfeld 2003; Ravichandran et al. 1999; Ullrich, Tanton, and Abdrashitova 2001).

Hg compounds can be split into two main subgroups: inorganic and organic. Inorganic forms of Hg are forms which do not contain carbon (C) such as elemental mercury [Hg(0)], mercuric sulphide (HgS) and mercuric oxide (HgO). These compounds are generally less bioavailable and therefore present a lower eco-toxicological hazard than organic compounds (Hoffman et al. 2002).

Inorganic speciation, such as HgO, are more readily deposited than Hg(0) via both wet and dry deposition due to their higher water solubility and chemical reactivity (United Nations Environmental Programme, Chemicals 2002). In Fenno-Scandinavian catchments deposition through litterfall after adsorption onto plant surfaces is a particularly important pathway for inorganic Hg to enter the ecosystem contributing approximately half of the Hg input to the forest floor (Johnson and Lindberg 1995; Munthe, Hultberg, and Iverfeldt 1995). Thus inorganic Hg compounds provide important pathways for atmospheric Hg to enter soils, and ultimately waters where they present the greatest hazard to human health (Bank, Loftin, and Jung 2005).

Organic forms of Hg contain C and tend to have a greater bioavailability, and thus eco-toxicity, than inorganic forms. Though a number of organic Hg compounds can occur naturally, the most commonly found compound is the monomethylated

mercury(II) cation[1] (MeHg) (Ullrich, Tanton, and Abdrashitova 2001). Methylation occurs when a methyl group (-CH_3) joins Hg to form $HgCH_3$. Methylation, and its inverse process, demethylation can both occur due to either abiotic or biotic processes depending on biogeochemical conditions such as redox, pH and the type of ligands available in the system (Gabriel and Williamson 2004; United Nations Environmental Programme, Chemicals 2002). The action of sulphate reducing bacteria (SRB) has been established to be principally responsible for methylation of Hg by a number of independent studies (Bergman et al. 2012; Compeau and Bartha 1985; Gabriel and Williamson 2004; Gilmour, Henry, and Mitchell 1992). SRB comprise the greatest proportion of the microbial community under reducing conditions, features such as peatlands, swamps and lake sediments are locations where the highest rates of methylation are observed.

MeHg is lipophilic and known to bioaccumulate in food chains with the highest concentrations being found in predatory fish and mammals (Zillioux, Porcella, and Benoit 1993). Mammals are estimated to uptake 95% of MeHg in Hg contaminated foods compared to 15% of elemental Hg contained in foods (Dietz et al. 2013). An important exposure pathway for humans in Sweden is via Hg contaminated food such as piscivorous fish (Åkerblom et al. 2014). Other exposure pathways exist, for example Hg0 volatalises readily to Hg vapour allowing it to be inhaled an absorbed through the lungs, however, elemental Hg is poorly absorbed through the gastrointestinal tract (Gochfeld 2003). Hg is toxic to humans with foetuses and infants being particularly vulnerable to Hg poisoning with exposure from the mother occurring during pregnancy or via breast milk (Dennis and Fehr 1975; Elghany et al. 1997; Trasande, Landrigan, and Schechter 2005). Symptoms include congenital birth defects, deficits in language acquisition, memory, motor skill development and the development of the immune system (Zahir et al. 2005). In adults, Hg poisoning is associated with neurodegenerative disorders such as Alzehimer's disease, Parkinson's disease and Amyotrophic Lateral Sclerosis (Zahir et al. 2005). A long-term epidemiological study into the effects of the Minamata Disaster[2] found significantly higher rates of hearing impairment, ataxia and hypoesthesia in inhabitants of fishing villages contaminated with Hg 10 years after a ban on the consumption of Hg contaminated fish (Ninomiya et al. 1995). The most severe cases of Hg poisoning lead to symptoms ranging from malaise and blurred vision at lower doses to causing ataxia, comas and ultimately death at the highest doses (Clarkson, Magos, and Myers 2003).

Hg also has negative effects on biota. Organic forms of Hg have been found to be between 10 and 100 times more toxic to plants and invertebrates compared to inorganic forms of mercury (Boening 2000). Aquatic invertebrates show adverse effects to the presence of Hg with Daphnia magna having a no effect exposure level (NOEL) of 3 μg/l and <0.04 μg/l for inorganic mercury and MeHg, respectively (Boening 2000). Hg has also been found to cause stress to plants, causing abnormal germination and hypertrophy of the root system (Patra and Sharma 2000).

[1] The monomethylated mercury(II) cation will be referred to as methylated mercury (MeHg).

[2] The Minamata disaster occurred in Minimata Bay, Japan during the 1950's when consumption of highly Hg contaminated sea produce led to severe Hg poisoning in the local populous (MacGregor and Clarkson 1974).

1.4 Mercury and dissolved organic carbon

Dissolved organic carbon (DOC) can be described as organic molecule which are able to pass through a filter sized 0.45μm (Kolka, Weishampel, and Fröberg 2008). DOC is heterogeneous in nature, consisting of organic molecules with differing chemical properties in varying amounts (Ravichandran 2004). Due to its chemical reactivity DOC can act as an important transport vector to allow Hg from terrestrial sources to move to aquatic environments. Approximately 60% of Hg observed in freshwaters is estimated to have originated from terrestrial sources (Lindqvist et al. 1991). Thiol (R-SH) groups found in the constituents of DOC such as humic and fulvic acids, have a higher complexation capacity for Hg (in the form of Hg^{2+} which is one of the softest Lewis acids (Wang and Zhang 2012) than for other competing metals such cadmium (Cd), zinc (Zn), copper (Cu) and lead (Pb) leading to preferential complexation with Hg (Skyllberg 2008; YANG et al. 2007). The strength of the correlation between DOC and Hg has been found to be more closely associated to the DOC quality rather than its quantity (Babiarz et al. 2003; Mierle and Ingram 1991; Ravichandran 2004). In a study of 19 Swedish watercourses Eklöf et al. (2012) found that organic matter fractions at Abs_{420} to be more important for Hg mobilisation than other fractions. This means that different DOC to Hg relationships can be seen within the same catchment according to the specific DOC quality. For example, within the same catchment a forested area may exhibit a different DOC to Hg relationship compared to a mire area.

In nutrient poor environments DOC may have a stimulatory effect on methylating microbes which may use the organic matter as a substrate and concert inorganic Hg to MeHg (Jackson 1989) and thus can affect the ratio of inorganic to organic Hg in a system. DOC also increases the solubility of Hg complexes facilitating transport through hydrological pathways. However, it should also be noted that complexed Hg is less likely to be methylated than Hg free in solution so DOC can also play a role in reducing MeHg content in water bodies (Gabriel and Williamson 2004). Whether or not DOC contributes to a net increase of Hg or MeHg flux will be dependent on a number of factors including: DOC quality, pH, redox, the microbial community and other ions present in the system (Wang and Zhang 2012).

1.5 Other influences on mercury mobilisation

Several other interrelated factors are relevant for Hg speciation, and therefore, mobilisation. The most important of these factors are: pH, dissolved ions and redox potential (Schuster 1991). Sulphur ions (S^-) are abundant at moderate to low redox conditions, in these conditions Hg is normally present as Hg(II) which readily binds to S^- to form HgS (Gabriel and Williamson 2004). HgS is virtually insoluble in water however in the presence of chloride ions (Cl^-) in concentrations of 3.5μL-1 its solubility can be increased by a factor of 408 (Gabriel and Williamson 2004). The effect of Cl^- ions in water which contains charged mineral surfaces such at goethite, is less clear. Various studies have concluded that dissolved ions have promoted, restricted or had no effect on complexation reactions (Langston and Bebianno 1998). The net effect of Cl^- will be dependent on pH and the other competing dissolved ions in the system. Fine sands will absorb MeHg at naturally occurring pH but

only at low concentrations of Cl^- where there is no competitive ion effect (Reimers and Krenkel 1974). 1:1 clays such as kaolinite are unable to form complexes with Hg whilst 2:1 clays with permanent charge such as illite are able to form strong complexes with Hg. Thus the composition of soils and sediments is important for Hg mobilisation and speciation (Reimers and Krenkel 1974). Illite forms complexes less readily in the presence of Cl^- and due to the amphoteric properties of clays, pH will determine whether the presence of a clay will raise or low the solubility of Hg and Hg compounds. Overall, the specific combination of conditions will determine whether soils and sediments act as Hg sinks or sources.

Once Hg is in the aqueous phase, site characteristics related to hydrology will determine whether this Hg will be able to reach stream water. Studies (Eklöf et al. 2014; Shanley and Bishop 2012) into the main drivers which control the movement of Hg from terrestrial sources to stream water have identified flow paths and hydraulic connectivity to be the dominant factor which control total Hg export.

1.6 Mercury in Sweden

In Sweden the majority of the Hg which is observed in stream water is transported from surrounding soils with the uppermost soil horizons containing the largest stores of Hg (Aastrup et al. 1991). A gradient in Hg contamination exist in Sweden with highest levels observed in the south and a declining trend towards the north of the country (Lindqvist et al. 1991; Åkerblom et al. 2014), however, Hg concentrations in all Swedish surface water bodies are currently at levels which causing them to fail the European Union's Water Framework Directive (WFD) (2000/60/EC) environmental quality standard (EQS) for Hg exposure to biota (European Commission 2012) and Hg concentrations in just over half of Swedish water bodies are in exceedance of FAO/WHO guidelines (Åkerblom et al. 2014). Hg levels in fish are also above the EU threshold value of 0.02 mg Hg kg^{-1} in most lakes (Kronberg 2014). Hg contamination in Sweden has been attributed to long-distance atmospheric transport (Munthe, Hellsten, and Zetterberg 2007). Atmospheric Hg is then deposited to soils through dry and wet deposition and bound in soil where it is eventually leached from soils (Demers, Driscoll, and Shanley 2010; Hintelmann et al. 2002; Munthe, Hellsten, and Zetterberg 2007). Hg from terrestrial sources is a key driver in Hg concentrations found in Swedish surface water bodies with lakes draining boreal forests typically receiving between 75% of Hgtot and 50% of MeHg from surrounding soils (K. H. Bishop and Lee 1997). Thus activities which impact the biogeochemical state of Swedish soils can be expected to have an impact upon Hg cycling.

Sweden has a large forestry sector that contributes a net of SEK 21.4 billion to the Swedish economy (Skogsstyrelsen [Swedish Forest Agency] 2014). A number of studies have highlighted a relationship between silviculture and Hg flux (Bishop et al. 2009; Eklöf et al. 2014; Munthe and Hultberg 2004; Porvari et al. 2003). Sørensen et al. (2009) estimated that somewhere between 10% and 25% of Hg in fish can be attributed to current silviculture practice. While a study conducted in Finland found that silviculture may increase net MeHg export by 400% in the first year after a clear-cut (Porvari et al. 2003).

Silviculture can increase the net export of Hg from an area by raising the water table and runoff quantity, runoff rate and hydrological connectivity (Bishop et al. 2009). Areas which have recently (< 5 years) been felled have higher rates of runoff

and higher water tables due to the decrease in plant transpiration (due to a reduction in vegetation) coupled with a decrease in surface roughness. Eklöf et al. (2014) found that although logging activities did not significantly increase Hg concentration, total export increase by between 50% - 70% due to the increase in discharge. Debris from forestry practices can provide a source of DOC which acts as transport vector for Hg, and also a source of good quality carbon that can promote net methylation. In addition to this the rise in water table can shift the source of water and associated dissolved constituents entering streams from the lower mineral horizon to the upper horizons. These upper horizons contain not only higher concentrations of Hg but also DOC with a greater proportion of aromatic compounds (Dittman et al. 2010). These conditions can promote net methylation rates as well as the transport of Hg to stream water depending on the specific biogeochemistry of the area.

However the extent of its effect on stream water concentrations of Hg will depend on a number of factors including site specific silviculture practice, climate, topography and the biogeochemistry of the area (Eklöf et al. 2014; Kronberg 2014).

2. Relevance and Objectives

Sweden's geographical position leaves it vulnerable to sources of Hg pollution from outside of its borders as evidence by an estimate 80% of atmospheric deposition originating from other countries (Lindqvist et al. 1991; Johansson, Bergbäck, and Tyler 2001). The podzolic soils which dominate Swedish forests are rich in negatively charged organic material which sorb deposited Hg allowing Hg to accumulate (Johansson, Bergbäck, and Tyler 2001). When this stored Hg is transported to water bodies it enters the food chain and biomagnifies through tropic levels. A number of studies conducted in Sweden have identified a link between the consumption of fish and Hg level within humans (Bárány et al. 2003; Lewerenz 1991; Wennberg et al. 2006). Thus to protect the well-being of both the human population and to safeguard the environment it is vital to be able to understand the mechanisms which control the cycling of Hg, especially the pathways which transport it from a position where it poses a relatively lower environmental hazards in soils, to a position where it can enter the food chain and ultimately end up in humans.

As DOC plays a key role as a transport vector for terrestrial Hg to enter water bodies, an understanding of its dynamics is crucial to being able to predict Hg cycling (French et al. 2014; Graham, Aiken, and Gilmour 2012; Åkerblom et al. 2008). Compared to Hg the dynamics of DOC are fairly well understood, some of this knowledge can be redeployed to increase understanding regarding Hg cycling. The Riparian Flow-Concentration Integration Model, has proven an effective tool to predict stream water DOC concentrations in a number of studies and more recently its effectiveness for model Hg dynamics has been tested.

This study aims to:

i. Identify and quantify trends within the Svartberget catchment pertaining to DOC, Hg_{tot} and MeHg fluxes.

ii. Provide a quantitative measure of the precision of the RIM model to predict stream DOC, Hg_{tot} and MeHg stream water concentrations.

iii. To inform theories as to which factors might be significant drivers for Hg_{tot} and MeHg flux through the examination of model residuals in the context of similar research.

iv. To suggest ways to improve the precision of the RIM model.

3. Materials and Methods

3.1 Catchment location and characteristics

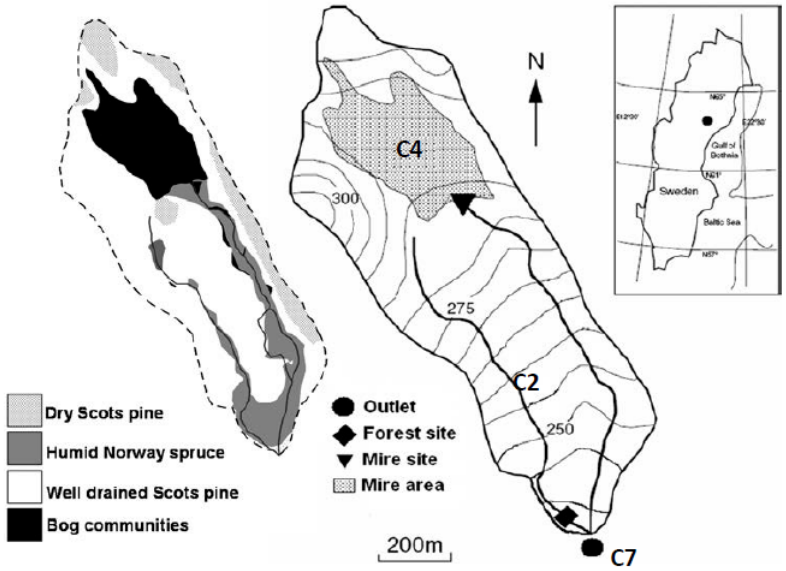

Figure 3.1: Map of Svartberget catchment showing study sites. Source: Oni et al. 2013.

The Svartberget catchment is located in 60 km to the west of Umeå in the province of Västerbotten, in the north of Sweden (64°14' N, 10°46' E) as seen in 3.1. The catchment spans 50 ha and drains headwaters from two streams, the Kallkällsbäcken (C7) and Västrabäcken (C2). The last site (C4) drains a mire. Most of the area is forested by mature (century old) Norway spruce (*Picea abies*) and Scots pine (*Pinus sylvestris*). Norway spruce is the dominant species in areas of higher elevation whilst in areas of lower elevation Scots pine is the dominant species (Laudon, Köhler, and Bishop 1999; Winterdahl et al. 2011). The exception to this a mire (C4) where vegetation is dominated by mosses (*Sphagnum* sp.) (Y. H. Lee et al. 1995).The soils are podzolic with a gneissic bedrock which is slow weathering and thus more susceptible to acidification, due to the reduced rate of atmospheric acid deposition these areas are considered to be recovering from acidification (Korsman 1999). Reduced levels of sulphur deposition (and therefore acidity) is thought to be contributing to the trend of increased DOC production in boreal catchments such as the study area (Monteith et al. 2007). Soil in the area is predominately well-developed ferric iron podzol which transitions into humic gleysols consists of 50 cm of organic-rich peat in the riparian zone (Cory et al. 2007). The area receives

610 ±109 mm/yr of precipitation annually with 35-50% of this coming in the form of snow (Köhler et al. 2008). On average the catchment is covered by snow for 170 days and the average air temperature is 1.7°C (Oni et al. 2013). Recent studies indicate that the area is recovering from sulphate deposition and an upward trend in air temperatures has been observed (Oni et al. 2013). The decrease in sulphate (and calcium) has been found to be contributing to a net decrease in the ionic strength of soil solution which could lead to more favourable conditions for DOC production and thus may also increase the rate of Hg_{tot} and MeHg export. The annual spring flood is the dominant hydrological event, peak flows are reached in April and May (figure A.2).

The riparian zone in upland forested part of the catchment (C2 and parts of C7) generally consist of well-developed pozolic soils which promote DOC production of approximately 50 cm depth, while the mire (C4) consists of soils which are generally 3-4 m in depth (Oni et al. 2013). In periods of low flow DOC concentrations in the mire subcatchment (C4) have been found to be higher than those in forested parts of the catchment (C2 and C7) with this situation being reversed during the annual spring melt (Ågren et al. 2008). Ågren et al. (2008) also found a layer of preferential flow in the wetland subcatchment at a depth of 2 – 2.5 m.

Site	Area (ha)	Forest (%)	Mire (%)	Till (%)	Tree volume (m^3 ha^{-1})	Spruce (%)	Pine (%)	Stand age (years)
C2	12	99.9	0.0	84.2	212	36	64	103
C4	18	55.9	44.1	22.0	83	45	55	57
C7	47	82.0	18.0	65.2	167	35	64	86

Table 3.1: Subcatchment characteristics. Adapted from Laudon et al. (2013).

3.2 Data gathering and analysis

A time series of data on flow and solute concentration (DOC, Hg_{tot}[3] and MeHg) was used in this study in combination with data from a soil transect where data on groundwater table and flow were collected. All data used in the study was collected by the Krycklan Catchment Study as part of a long-term monitoring programme.

Seasonal and long-term trends were assessed using the Mann-Kendall (MK) trend test, the Mann-Kendall test is a non-parametric test which makes no assumptions in the distribution of data (Hamed and Ramachandra Rao 1998). This makes it suitable for examining trends in DOC, Hg_{tot} and MeHg across multiple sites where information regarding the distribution of the data is unknown. This method has also been employed in previous studies into temporal trends within the Svartberget catchment which will allow for the results to be more easily compared (Winterdahl et al. 2011). The MK trend test null hypothesis is that both series X and series Y are ordered independently, it is defined as follows. For two sets of observations in the form $X = x_1, x_2, \ldots, x_n$ and in a similar fashion for Y. The S statistic is

[3]No data was available for Hg_{tot} at site C4

calculated using equation 3.1:

$$S = \sum_{i<j} a_{ij} b_{ij} \tag{3.1}$$

The term a_{ij} is defined in equation 3.2:

$$a_{ij} = sgn(x_j - x_i) = \left\{ \begin{array}{rrcl} 1 & x_i & < & x_j \\ 0 & x_i & = & x_j \\ -1 & x_i & > & x_j \end{array} \right\} \tag{3.2}$$

The term b_{ij} is defined similarly, replacing x_i for y_i and x_j for y_j. Y values are replaces with the order of the time series for trend analysis. Significance is tested by selecting the desired p-value and comparing the standardised test statistic with the standard normal variate (Hamed and Ramachandra Rao 1998). Monthly means of raw data were used as inputs to the MK test. The Nash-Sutcliffe efficiency index (NSE) was used to assess model performance, with a values of ≥ 0.20 classed as been behavioural. The NS efficiency index is defined in equation 3.3 (Schaefli and Gupta 2007):

$$NSE = 1 - \frac{\sum_{t=1}^{N} [q_{obs}(t) - q_{sim}(t)]^2}{\sum_{t=1}^{N} [q_{obs}(t) - \bar{q}_{obs}]^2} \tag{3.3}$$

NSE has a domain of $-\infty$ to $+1$, with a perfect simulation attaining a value of $+1$. If simulated values are worse than using the mean to predict the value of observations the NSE will be less 0.

Model performance was measured using the following:

i. The coefficient of determination (R^2) between modelled values and observed data. This value represents the proportion of variance in modelled data explained by the model (Nagelkerke 1991).

ii. The mean squared error (MSE) and the median square error (MedAE) which is the average squared distance between the modelled value and the observed value (Wallach and Goffinet 1989).

Data exploration, cleaning and preliminary analysis was conducted using an Enthought® Canopy distribution of Python, basic statistics (mean, standard error etc.), analysis of correlation and modelling were carried out using JMP® Pro 11 and Microsoft® Excel.

3.3 The Riparian Integration Flow-Concentration Model

The Riparian Integration Flow-Concentration Model (RIM) allows the calculation of stream concentrations of chemical parameters through linking soil concentration and flow though the soil pore interspace. It is grounded in some important assumptions:

i. Concentrations of solutes in water laterally traversing the riparian zone become influenced by the chemical signature the soil at that particular depth (K. Bishop et al. 2004). The soil thus acts as a chemostat; water leaving a soil will have the chemical fingerprint of the soil through which it passed.

ii. The riparian soil can be split into an infinite number of horizontal layers. The solute concentration of water travelling from soil to stream will be the sum of all layers below it i.e. the integral of the relationship between depth and solute concentration.

Using these two basic assumptions and data regarding the relationship between how flow causes groundwater table (GWT) depth to vary, the model can be calibrated to the hydrological properties of a soil. In cases where simultaneous measurement of both flow and stream water solute concentration exist, the calibration process can be repeated to establish the relationship between flow and stream water solute concentration.

The RIM model is defined in equation 3.4 as presented by previous research (Seibert et al. 2009; Winterdahl, Futter, et al. 2011):

$$L = \int_{z_0}^{z_1} ae^{bz} \mathrm{c0} e^{fz} \mathrm{d}z \tag{3.4}$$

Where z is depth, $c0$ is the initial solute concentration at the soil surface and a, b, f are parameters. The terms ae^{bz} describes the hydrology of the medium through which water is passing. Performing linear regression between flow and GWT in log-linear space and taking the derivative of this result allows integration using equation 3.7.

The relationship between flow and depth to the groundwater table will allow simulation of the GWT depth for any given flow. Thus if stream water concentrations are known for a series of different flow rates, a relationship can again be established. The term $c0e^{fz}$ describes the relationship between depth in the soil profile and expected stream water concentration.

This means that after the RIM model has been calibrated, it can then be used to simulate expected stream water concentrations for a given solute. The conceptual relationship linking flow, GWT depth and solute concentration is presented in figure 3.2.

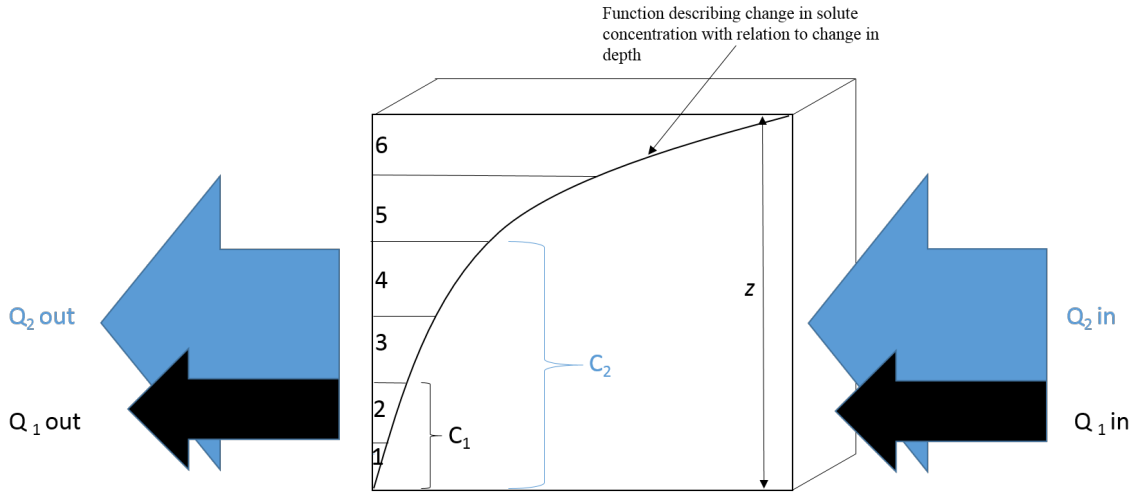

Figure 3.2: Conceptual description of the relationship between flow (Q), depth (z) and solute concentration (C). $C1$ and $C2$ will be equal to the sum of layers 1-2 and 1-5, respectively.

3.4 The analytical solution to the RIM model

The analytical solutions to the RIM model can be calculated through by integrating over stream flow and using the following steps as presented by Seibert et al. 2009:

i. Substitute the profile depths for stream flow and rewrite the equation:

$$z = b^{-1} \ln(\frac{bQ}{a}) \tag{3.5}$$

$$\mathrm{d}z = (bQ)^{-1} \mathrm{d}Q \tag{3.6}$$

ii. Set the lower integration limit to negative infinity, this will mean that the lower limit for stream flow will be 0 after the substitution in step (i).

$$L = aC0 \int_{-\infty}^{z_1} e^{(b+f)z} \mathrm{d}z \tag{3.7}$$

iii. Introduce a new parameter to represent a power-law $\omega = \frac{b+f}{b}$, ω:

$$L = c0 \frac{(\frac{a}{b})^{1-\omega}}{\omega} Q^{\omega} \tag{3.8}$$

3.5 Model parameterisation

Nonlinear least squares was used to calculated parameter estimates using the Levenberg-Marquardt algorithm as described by Moré (1978). The algorithm was implemented through the SciPy library written in the Python programming language (Jones, Peterson, and et al. 2014).

Observed simultaneous measurements of the depth to the GWT and flow were used as target data to establish the hydrological parameters of RIM. The objective function to minimise is presented in equation 3.9:

$$Y = ae^{bz} \tag{3.9}$$

Where a and b are parameters and z is depth in soil profile. As no soil solution profile data was available the chemical parameters of the RIM model were set directly between (simulated) GWT depth and observed stream water concentrations. The objective function to minimise is presented in equation 3.10:

$$Y = c0e^{fz} \tag{3.10}$$

Where *c0* and f are parameters and z is depth in soil profile. Parameter estimates for functions can be seen in table 4.3.

3.6 Limitations of the RIM_{static} model and other versions of RIM

The RIM_{static} model has been able to produce statistically significant predictions for the solute concentrations and fluxes in the number of previous studies (Seibert et al. 2009; Winterdahl et al. 2011). However, due to the nature to the model and the assumptions on which it is based some areas of weakness have been identified. This has led to the development of variation of the standard static RIM model, RIM_{static} and its modification to form dynamic version of the RIM model.

There are three versions of dynamic RIM, RIM_{dyn}c0, RIM_{dyn}f and RIM_{dyn}c0+f. In $RIM_{dyn}c0$ the $c0$ term (the initial concentration) of equation 3.4 is varied, in $RIM_{dyn}f$ the f term (the slope gradient or growth rate, for log and linear forms of RIM, respectively) and $RIM_{dyn}c0 + f$ where both the $c0$ and f terms are allowed to vary.

The changing biogeochemical conditions within the soil profile alter a characteristics with regards to DOC, Hg and MeHg production. These process are not taken into account by RIM_{static} which is driven by flow; a given flow will always produce the model value for stream water solute concentration. The RIM_{static} model will predict a value which is the average between peaks and troughs of seasonal variation and thus modelled values will systematically under and over predict observed concentrations.

Winterdahl et al. (2014) found that variability in DOC trends on annual timescales was influenced by a number of characteristics. Key drivers other than flow were found to be month and temperature, with the relative importance of these drivers varying considerably between catchments.

The dynamic versions of RIM_{static}, RIM_{dyn} attempt to account for seasonality through the use of a sine wave to modulate either or both of c0, the initial concentration or f, the fitting factor. When RIM_{static} and RIM_{dyn} have been applied to the same dataset, RIM_{dyn} shows improved predictive power as measured by the Nash-Sutcliffe model efficiency coefficient (NS) (Winterdahl et al. 2011). Whilst the use of a sine wave can help to simulate seasonality it also has limitations. If trends do not display symmetry in the modulations around their mean (or other constant baseline) the dynamic RIM model will vary either too quickly or too slowly and limiting its performance. The rate of seasonal change within a season is often not constant (e.g. spring floods vs winter months) which could lead to the sine function

modulating the RIM function at too great or to slow a rate a points throughout a year.

A novel dynamic version of the RIM_{static} model, RIM_{med} (RIM median) is proposed and will be compared to simulations by RIM_{static} and $RIM_{dyn}c0$[4]. RIM_{med} assigns a value to each calendar month based on the median of that month's distance from the median of the whole dataset. The rationale is to assign each month a seasonal value which will be used to modulate modelled output based on the month in which the prediction occurs. This will allow for a more responsive and flexible modulation of simulated values. The conceptual difference between RIM_{static}, RIM_{dyn} and RIM_{med} can be seen in figure 3.3.

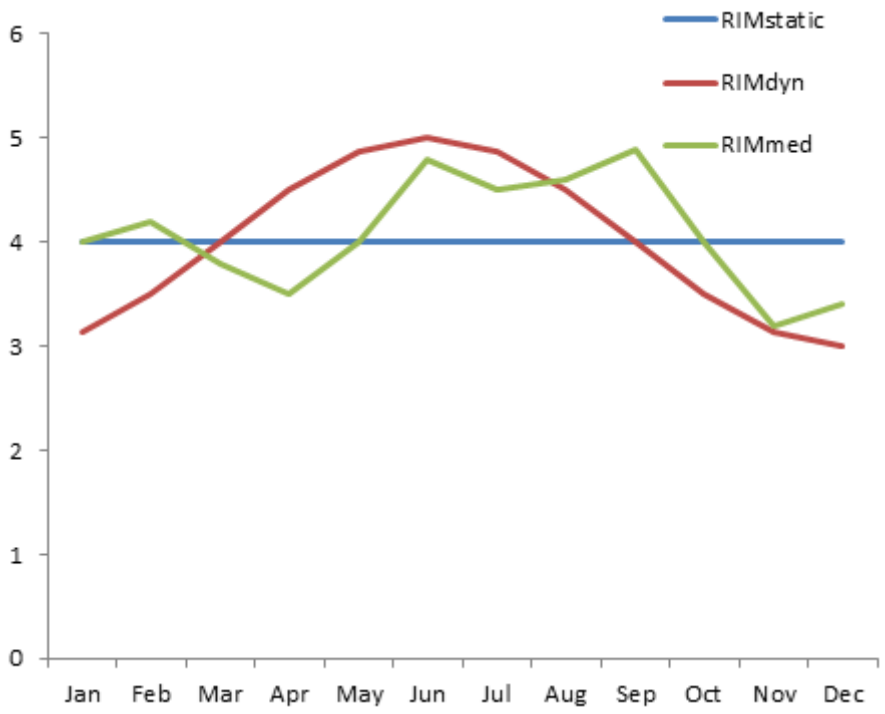

Figure 3.3: Depiction of the conceptual differences between RIM_{static} (blue), RIM_{dyn} (red) and RIM_{med} (green).

[4]Herein referred to as RIM_{dyn}

4. Results

4.1 Solute concentration trends

4.1.1 DOC stream concentration trends

Visual inspection of DOC stream water trends showed a near constant trend across all sites, this was confirmed by positive Sen's slope value and small positive τ-values (table 4.2). However this trend was only statistically significant at sites C2 and C4 (table 4.2).

The mean DOC concentration over the study period was 31.81 ±0.55 mg/L, 14.62±0.39 mg/L and 20.52 ±0.32 mg/L for sites C2, C4 and C7, respectively (table 4.1). Peak months for DOC concentration occurred in: March for site C2 (39.13 ±1.27 mg/L), August for site C4 (21.92 ±1.78 mg/L) and October for site C7 (24.89 ±1.16 mg/L) (figure 4.1 a, c, e).

The seasonal Mann-Kendall trend test identified a stronger and more statistically significant trend as sites C2 and C7 compared to the Mann-Kendall trend test which does not take into account seasonality however the opposite effect was observed at site C4.

All sites showed weak correlation between DOC stream water concentration and GWT depth with sites C4 and C7 showing negative correlation and site C2 showing a positive correlation (table A.2, figure 4.2).

	Site	n	Min	Max	Mean	Median	Standard error	Standard deviation
DOC mg/L	C2	381	8.25	62.00	31.81	32.10	0.55	10.74
	C4	328	3.60	52.50	14.62	13.10	0.39	7.11
	C7	433	7.10	43.00	20.51	19.80	0.32	6.70
Hg_{tot} ng/L	C2	0	-	-	-	-	-	-
	C4	50	2.09	11.24	4.65	4.36	0.21	1.87
	C7	66	2.93	13.50	4.68	4.07	0.27	2.48
MeHg ng/L	C2	46	0.03	0.87	0.20	0.14	0.02	0.17
	C4	54	0.02	2.94	0.65	0.47	0.05	0.63
	C7	71	0.01	0.98	0.36	0.38	0.02	0.21

Table 4.1: Summary statistics for DOC, Hg_{tot} and MeHg by site

	Site	MK	P	Sen's slope	Seasonal MK	Seasonal P	Seasonal Sen's slope	Seasonal MK minus MK
DOC mg/L	C2	0.060	0.079	0.009	0.079	0.032	0.144	**0.019**
	C4	0.119	0.001	0.013	0.117	0.003	0.150	-0.002
	C7	0.049	0.129	0.004	0.063	0.061	0.062	**0.014**
Hg_{tot} ng/L	C2	-	-	-	-	-	-	-
	C4	0.134	0.06	0.013	0.175	0.062	0.208	**0.041**
	C7	0.046	0.491	0.004	0.077	0.372	0.173	**0.031**
MeHg ng/L	C2	-0.354	<0.0001	-0.003	-0.37	0.002	-0.019	**-0.016**
	C4	-0.105	0.128	-0.002	-0.152	0.074	-0.031	**-0.047**
	C7	-0.171	0.007	-0.002	-0.258	0.001	-0.026	**-0.087**

Table 4.2: Comparison of τ-values, P-values and Sen's slope for non-seasonal and seasonal Mann-Kendell trend test. α was set at 0.05. Bold values indicate a stronger correlation in the seasonal Mann-Kendell trend test over non-seasonal.

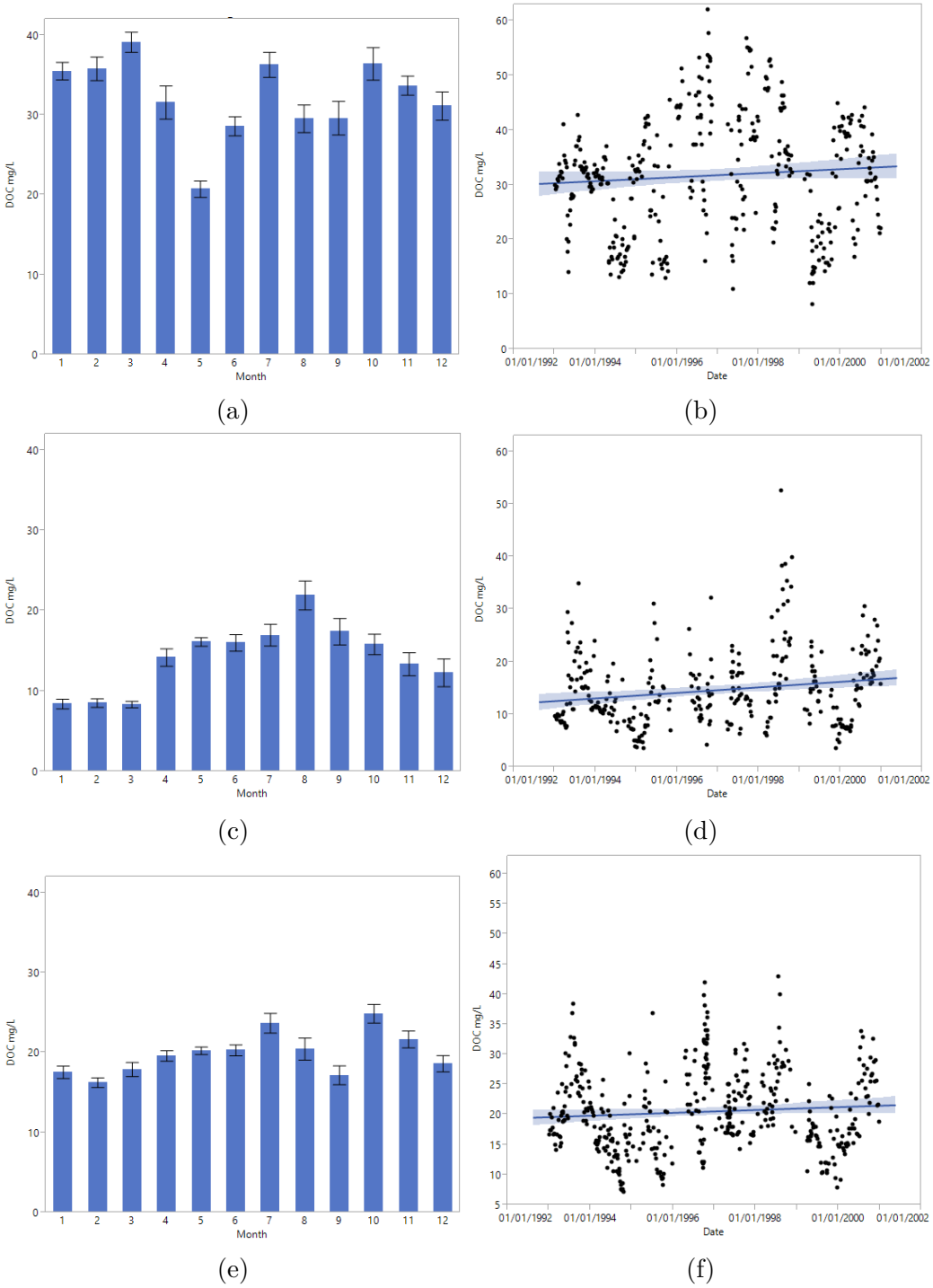

Figure 4.1: (Left) Bar charts showing DOC stream water concentration monthly means and error bars for sites C2 (a), C4 (c) and C7 (e). (Right) DOC time series with line of best fit (blue) and confidence of fit (shaded blue) for sites C2 (b), C4 (d) and C7 (f).

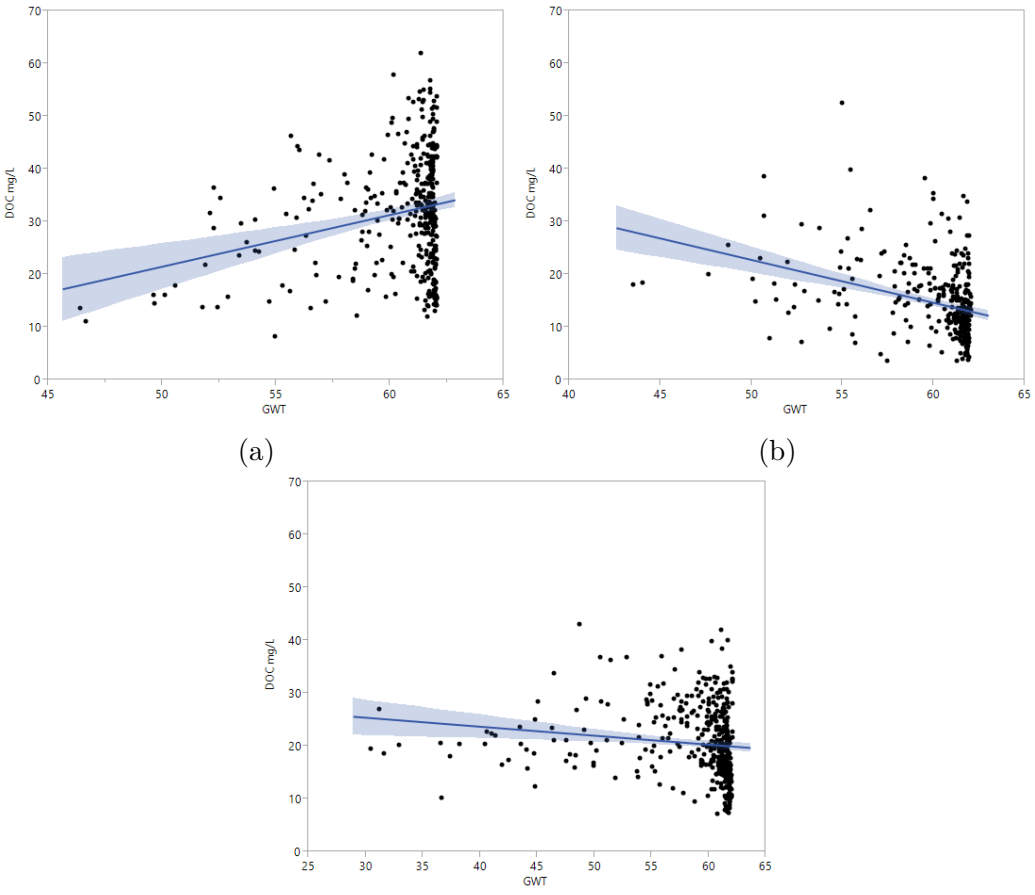

Figure 4.2: Scatter plots of DOC mg/L against GWT depth in cm with a line of best fit (blue) and confidence of fit (light blue) for sites C2 (a), C4 (b) and C7 (c).

4.1.2 Hg_{tot} stream water concentration trends

Hg_{tot} stream water concentrations had a near constant trend during the study period (figure 4.3 (b), (d)). The Mann-Kendall trend test for both site did not have statistical significance thus the null hypothesis, that no trend exists, cannot be rejected.

The mean Hg_{tot} stream water concentration was 4.36 ±0.21 ng/L and 4.07 ±0.27 ng/L for sites C4 and C7, respectively. Peak months for Hg_{tot} concentration occurred in June for site C4 (5.52 ±1.04 ng/L) and site C7 (6.91 ±01.52 ng/L) (figure 4.3, (a), (c)). Hg_{tot} appeared to display seasonal trends in both sites with the period of highest stream concentration occurring in May and June, this trend was more pronounced in site C4 (figure 4.3, (a)).

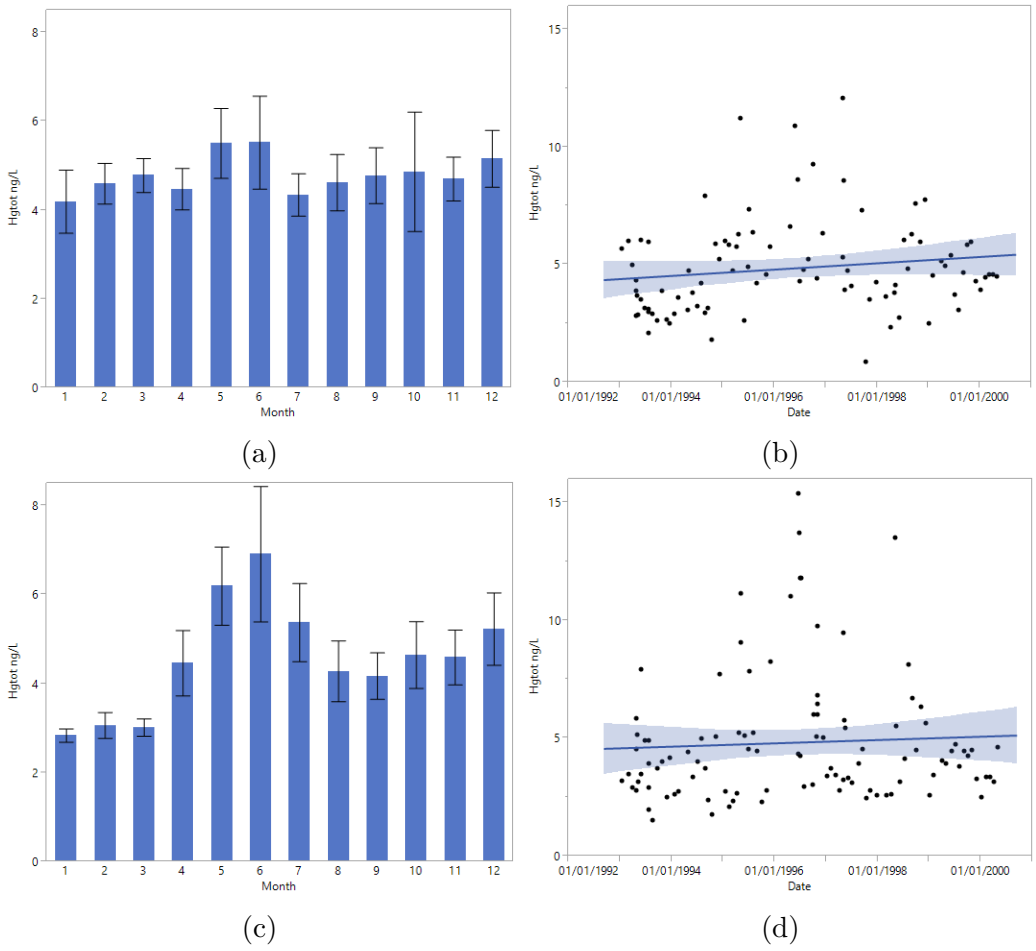

Figure 4.3: (Left) Bar charts showing Hg_{tot} ng/L stream water concentration monthly means and error bars for sites C4 (a) and C7 (c). (Right) Hg_{tot} ng/L stream water concentration time series with line of best fit (blue) and confidence of fit (shaded blue) for sites C4 (b) and C7 (d).

4.1.3 MeHg stream water concentration trends

MeHg stream water concentrations appear to have a slight downward trend over the study period (figure 4.4, (b), (d), (f)), this was confirmed by negative τ-values and a Sen's slope with a negative gradient as all sites however the Mann-Kendall

trend test only had statistically significance at sites C2 and C7 (table 4.2). The mean stream water concentration was 0.20 ±0.02 ng/L, 0.65 ±0.05 ng/L and 0.36 ±0.02 ng/L for sites C2, C4 and C7, respectively (table 4.1). Peak months for MeHg stream water concentration occurred in: February for site C4 (1.64 ±0.44 ng/L) and August for sites C2 (0.56 ±0.18 ng/L) and C7 (0.56 ±0.12 ng/L) (figure 4.4 (a), (c), (e)).

All sites appear to be influenced by seasonal processes with the seasonal Mann-Kendall trend test producing stronger correlation than the non-seasonal test (table 4.2). Sites C2 and C4 both have one large annual spike, in August and February, respectively, whilst at site C7 this spike is less pronounced (figure 4.4 (a), (c), (e)).

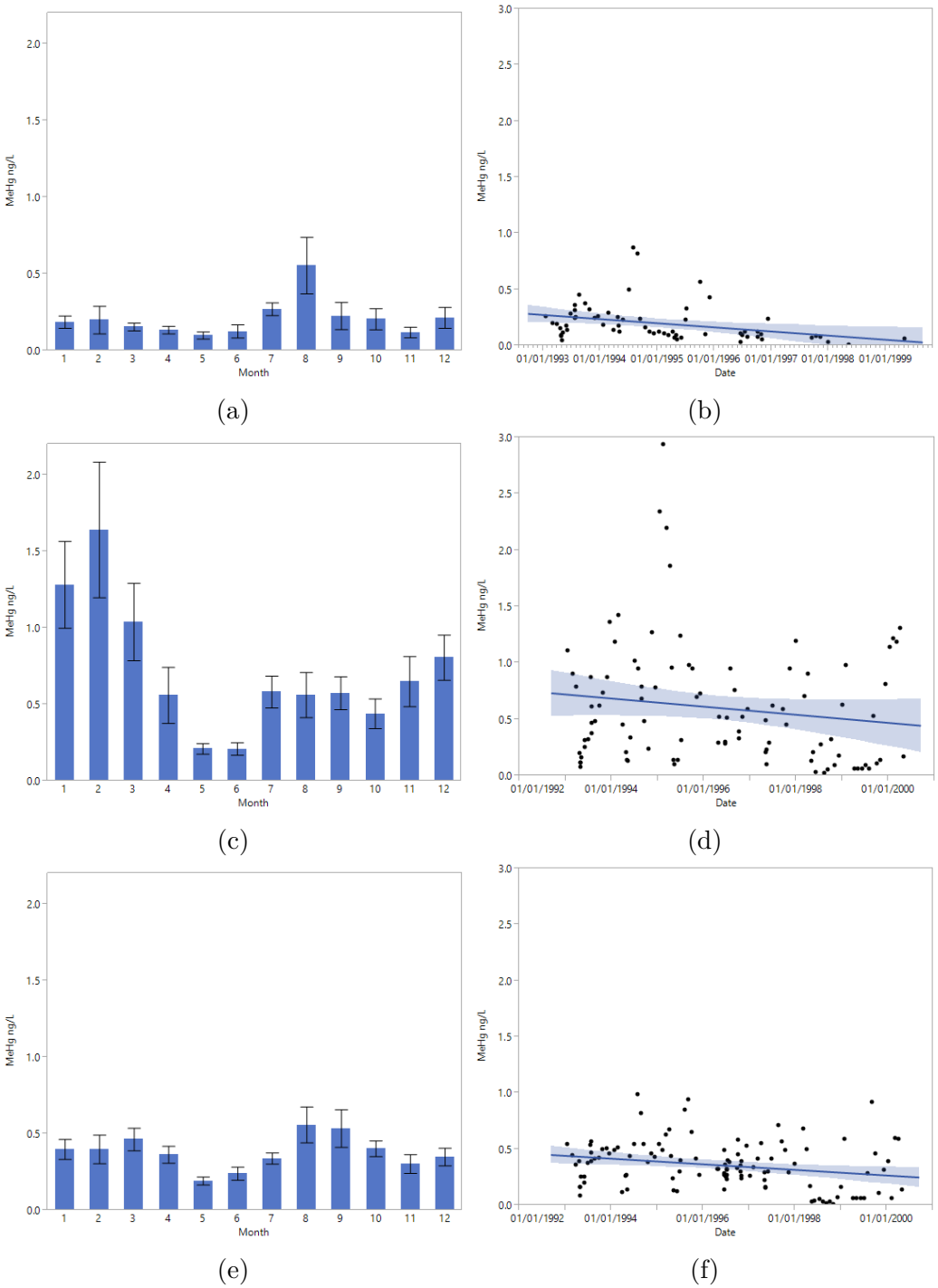

Figure 4.4: (Left) Bar charts showing MeHg stream water concentration monthly means and error bars for sites C2 (a), C4 (c) and C7 (e). (Right) MeHg time series with line of best fit (blue) and confidence of fit (shaded blue) for sites C2 (b), C4 (d) and C7 (f).

4.2 RIM simulations

4.2.1 Hydrological parameters

Hydrological parameters were set using GWT depth at varying flow rates. The logs of the data were plotted and linear regression was used to establish the relationship between flow rate and depth to the GWT (figure 4.5). There was a strong negative correlation between flow rate and GWT depth ($R^2 = 0.93$, $P = \pm 0.0001$). The y-intercept ($c0$) was log 4.11 cm and the slope was log -0.16.

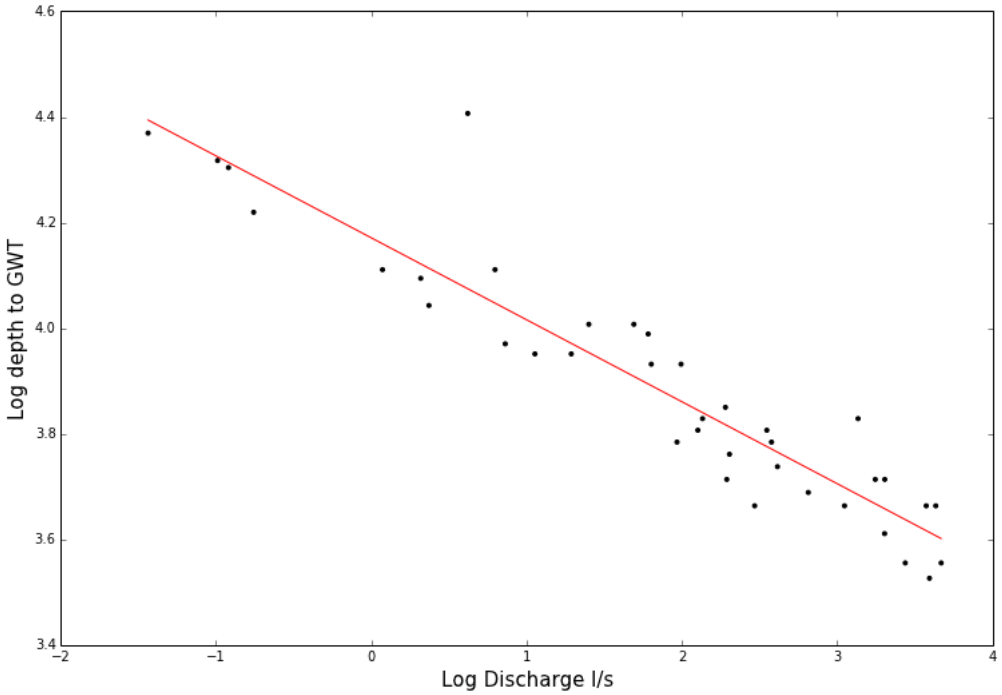

Figure 4.5: Linear regression of the logs of depth to groundwater table (cm) against flow rate (L/s). Measurements were taken at site C4.

4.2.2 Chemical parameters

The procedure for establishing the hydrological parameters was used to model the GWT depth for all flow data points. This data was then used in conjunction with solute concentrations to establish the relationship between GWT depth and stream water concentrations. The process was repeated for each solute (DOC, Hg_{tot} and MeHg) at each site (C2, C4, C7), parameter estimates and goodness-of-fit metrics can be seen in table 4.3.

	Site	R^2	RMSE	Parameter estimates			
				a	Standard error	b	Standard error
DOC mg/L	C2	0.054	10.464	4.504	2.194	0.032	0.008
	C4	0.108	6.728	170.122	60.067	-0.041	0.006
	C7	0.017	6.650	31.009	4.646	-0.007	0.003
Hg_{tot} ng/L	C2	-	-	-	-	-	-
	C4	0.020	2.013	1.546	1.408	0.019	0.015
	C7	0.023	2.705	10.018	4.464	-0.013	0.008
MeHg ng/L	C2	0.028	0.168	0.006	0.019	0.058	0.054
	C4	0.118	0.501	0.000	0.000	0.163	0.074
	C7	0.063	0.203	0.063	0.052	0.030	0.014

Table 4.3: Correlation, root mean squared error and parameter estimates for parameters a and b. Values rounded to 3 decimal places.

4.2.3 DOC simulations

Sites C4 ($R^2 = 0.108$, RMSE = 6.728) and C7 ($R^2 = 0.017$, RMSE = 6.650) both showed a negative correlation between DOC stream water concentration and depth to the GWT (figure 4.6, (b) and (c)). Site C4 ($R^2 = 0.054$, RMSE = 10.464) showed a positive relationship between DOC stream water concentration and depth to the GWT (table 4.3 and figure 4.6, (a)). Parameter estimates for fits can be seen in table 4.3.

Poor results in goodness-of-fit metrics seen in table 4.3 suggest that the function used to model the relationship ($c0e^{fz}$) between DOC stream water concentration may not have been optimal.

RIM_{med} simulations showed the best model performance across the metrics used to assess model performance with NSEs of 0.214 (C2), 0.297 (C4) and 0.138 (C7) (table 4.4). Both RIM_{dyn} and RIM_{med} appeared to model seasonal variation better than RIM_{static} as evidenced by higher NSE and a closer fitting graph when plotted against observed measurements (figure 4.7).

	Site	RIM_{static}			RIM_{dyn}			RIM_{med}		
		NSE	MAE	MedAE	NSE	MAE	MedAE	NSE	MAE	MedAE
DOC mg/L	C2	0.054 (<0.001)	8.473	7.958	0.040 (<0.001)	8.613	7.891	0.214 (<0.001)	7.513	5.857
	C4	0.108 (<0.001)	5.073	3.985	0.254 (<0.001)	4.572	3.828	0.297 (<0.001)	4.359	3.300
	C7	0.017 (0.006)	5.375	4.738	0.030 (<0.001)	5.392	4.663	0.138 (<0.001)	4.744	3.491
Hg_{tot} ng/L	C2	-	-	-	-	-	-	-	-	-
	C4	0.020 (0.183)	1.463	1.048	0.031 (0.091)	1.496	1.177	0.031 (0.096)	1.440	1.163
	C7	0.023 (0.125)	1.902	1.462	0.075 (0.005)	1.949	1.531	0.134 (<0.001)	1.823	1.272
MeHg ng/L	C2	0.028 (0.186)	0.120	0.098	0.132 (0.003)	0.118	0.107	0.393 (<0.001)	0.106	0.082
	C4	0.118 (0.001)	0.359	0.268	0.244 (<0.001)	0.355	0.309	0.387 (<0.001)	0.320	0.244
	C7	0.063 (0.007)	0.158	0.124	0.030 (<0.001)	0.170	0.150	0.264 (<0.001)	0.142	0.114

Table 4.4: Nash-Sutcliffe efficiencies (P-values), mean average error and median average error for RIM_{static}, RIM_{dyn} and RIM_{med} for DOC, Hg_{tot} and MeHg at all sites. Values rounded to 3 decimal places.

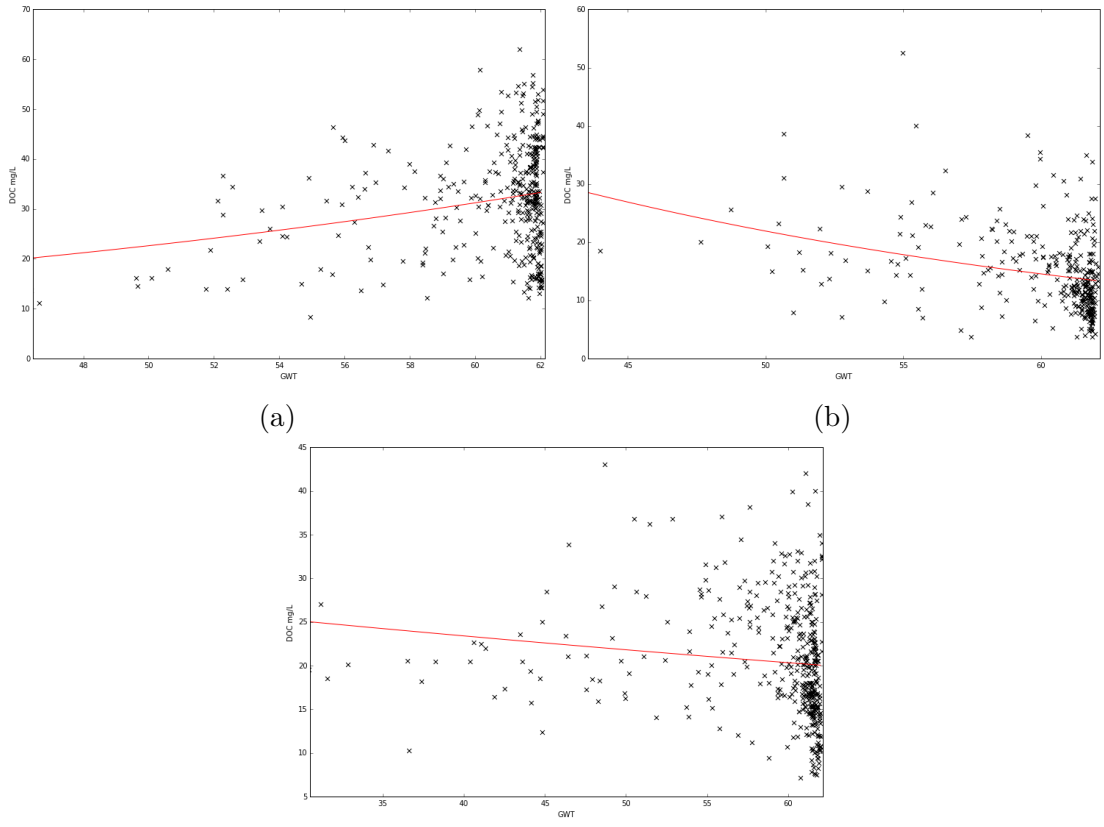

Figure 4.6: Nonlinear regression of DOC concentration (mg/L) against depth to groundwater table (cm). At sites C2 (a), C4 (b) and C7 (c).

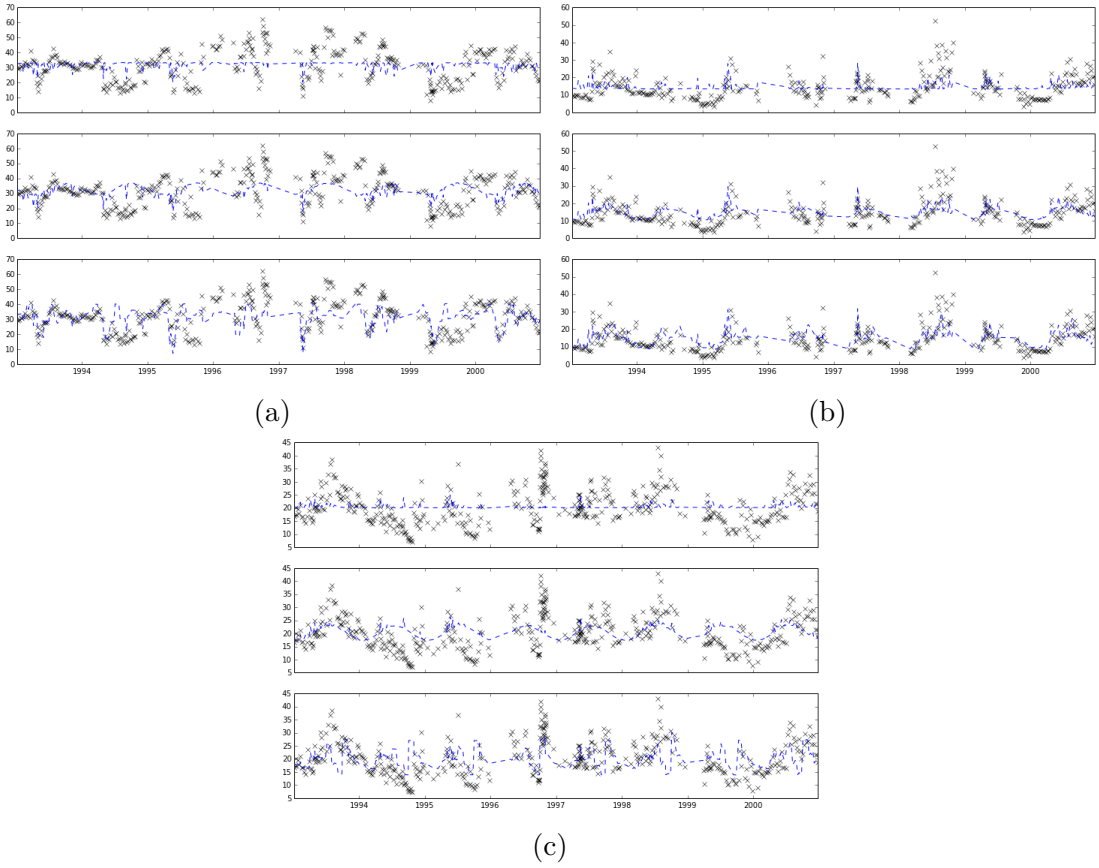

Figure 4.7: Time series of observed stream water DOC concentration (mg/L) (black crosses) with simulated values (blue dashed line). For RIM_{static} (top), RIM_{dyn} (middle) and RIM_{med} (bottom) at sites C2 (a), C4 (b) and C7 (c).

4.2.4 Hg_{tot} simulations

None of the models tested were classed as functional for simulating Hg_{tot} stream water concentrations at sites C4 or C7 (table 4.4). RIM_{med} outperformed other versions of RIM with NSEs of 0.031 (P= 0.096) and 0.134 (<0.001) and for sites C4 and C7, respectively (table 4.4).

No version of RIM was able to adequately simulate the range of stream water concentrations which could be produced at a given GWT depth (figure 4.8). Modelled values overestimated low Hg_{tot} stream water concentrations while underestimating high Hg_{tot} stream water concentrations (figure 4.9).

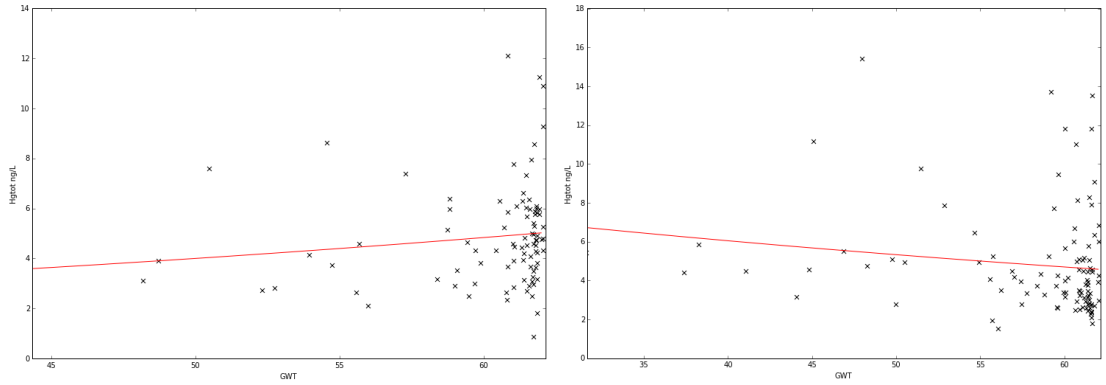

(a) (b)

Figure 4.8: Nonlinear regression of the Hg_{tot} concentration (mg/L) against depth to groundwater table (cm). At sites C4 (a) and C7 (b).

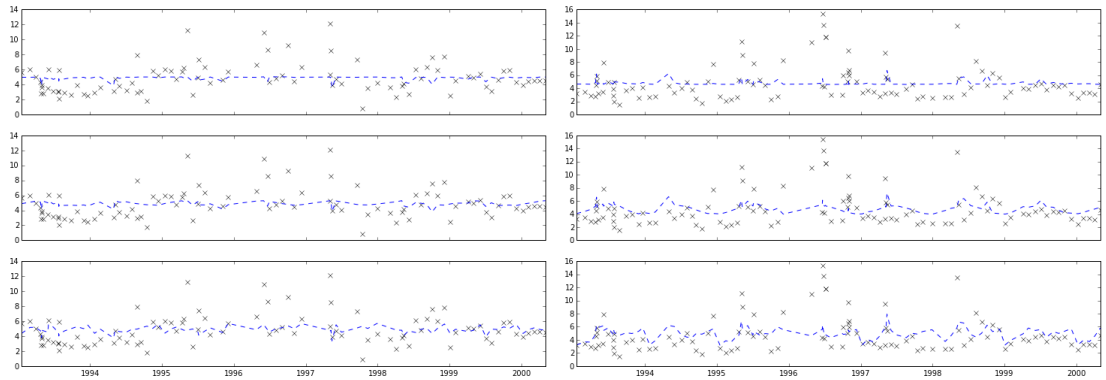

(a) (b)

Figure 4.9: Time series of observed stream water Hg_{tot} concentration (ng/L) (black crosses) with simulated values (blue dashed line). For RIM_{static} (top), RIM_{dyn} (middle) and RIM_{med} (bottom) at sites C4 (a) and C7 (b).

4.2.5 MeHg simulations

RIM_{med} was classified as functional across all sites with NSEs of 0.393 (<0.001), 0.387 (<0.001) and 0.264 (<0.001) at sites C2, C4 and C7, respectively. RIM_{dyn} was classified as functional at site C2 only with an NSE of 0.244 (<0.001), while RIM_{static} was not functional at any site (table 4.4).

MeHg dynamics appear to be governed by flow, with periods of low flow (i.e. large depth to GWT) producing the highest stream water concentrations (figure 4.10).

Seasonality for MeHg did not appear to follow a regular pattern and low flows were able to produce a wide range of stream water concentrations (figure 4.10). Analysis of model residuals showed that much of the model error occurred at high GWT depths (i.e. low flows), where the same flow rate was capable of generating varying levels to stream MeHg concentrations (figure A.6). This lead to periods when all models failed to simulate MeHg stream water concentrations correctly (figure 4.11). Soil temperatures with a moving average of the previous 30 days were plotted against MeHg stream concentrations (figure A.1). A significant positive trend was found at sites C4 (R^2 = 0.426, P = <0.001) and C7 (R^2 = 0.233, P = <0.031) (table A.1).

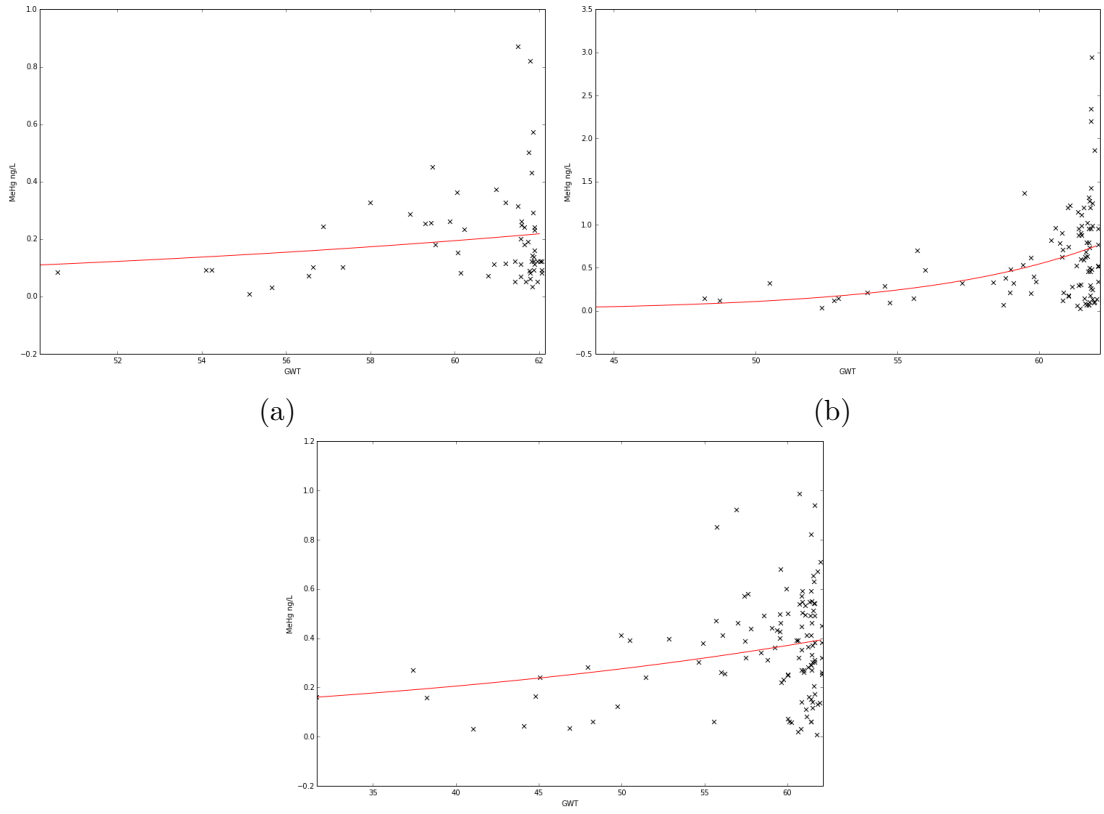

(a) (b)

(c)

Figure 4.10: Nonlinear regression of the MeHg concentration (mg/L) against depth to groundwater table (cm). At sites C2 (a), C4 (b) and C7 (c).

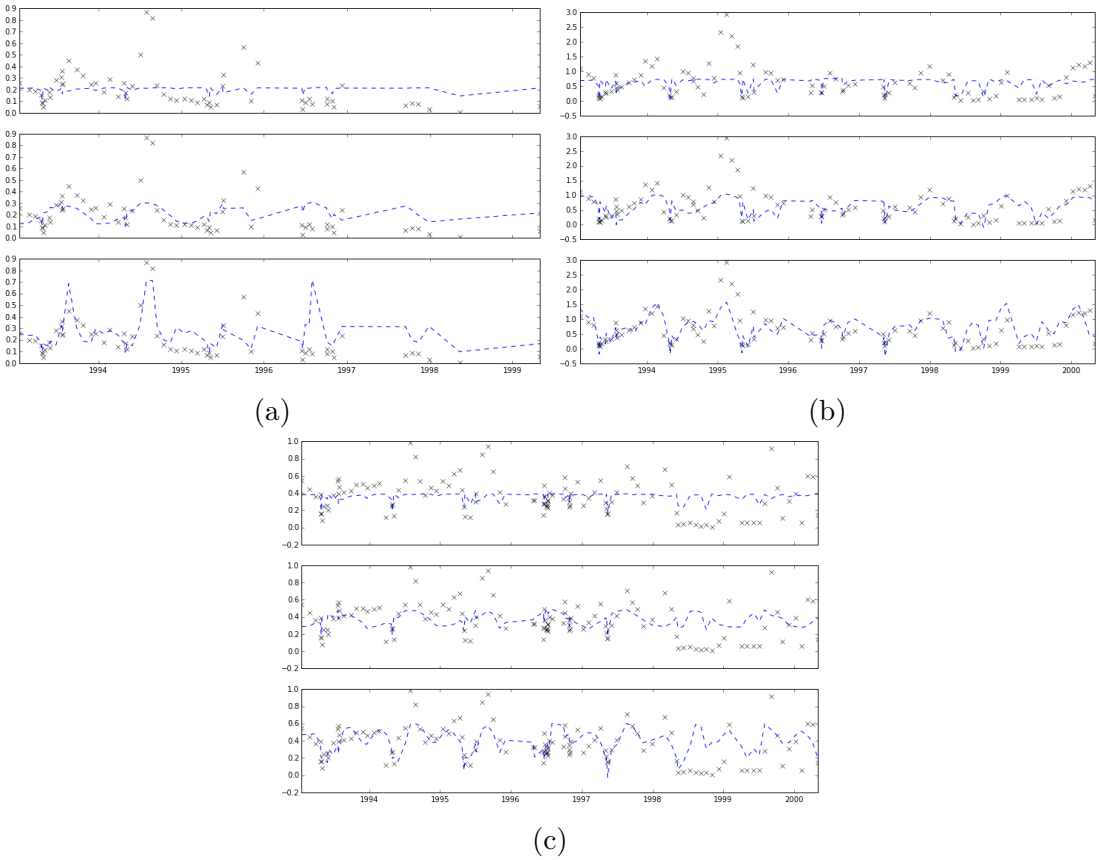

Figure 4.11: Time series of observed stream water MeHg concentration (ng/L) (black crosses) with simulated values (blue dashed line). For RIM_{static} (top), RIM_{dyn} (middle) and RIM_{med} (bottom) at sites C2 (a), C4 (b) and C7 (c).

5. Discussion

5.1 Trend analysis: spatial and temporal variation

The steady to slight increasing trend found in DOC stream concentrations on an annual basis (table 4.2) is consistent to previous research conducted within the Svartberget catchment (Monteith et al. 2007; Oni et al. 2013; Winterdahl et al. 2011) and in a similar study in Finland (Sarkkola et al. 2009). However, this may be due to an insufficient of study. In a long-term trend analysis of the Svartberget catchment, Oni et al. (2013) found that due to warmer temperatures, a longer growing season and a decline in snowpack, the precipitation regime has shifted from high intensity annual flash flood events to small more frequent flushing events. These smaller more regular flushing events are more conducive to DOC production. Oni et al. (2013) also found evidence to suggest that flushing of the upper layers of the soil profile were a more important flow pathway than transport through subsurface layers in groundwater.

Previous research has established strong negative relationship between the amount of sulphur deposition and DOC production (Clark et al. 2010). Clark et al. (2010) found that DOC production can vary even in areas receiving the same input due to different catchment characteristics and that the magnitude of effects for a certain input varied both in time and scale. This explains why the three sites examined in Svartberget, C2, C4 and C7 can display such heterogeneity both between each other and inter-annually. Despite their geographical proximity, the local conditions are very different (forest-based, mire and mixed) from one another and this is reflected in their different behaviour in terms of solute concentrations.

Yurova et al. (2008) applied the convection-dispersion equation model to a boreal mire in northern Sweden to simulate DOC concentrations. The study found that conditions in previous seasons, as far back as 5 years, affected the chemistry of the catchment in subsequent seasons these findings were replicated in another study by Köhler et al. (2009). This would offer a potential explanation the results in this study, where the same flow rate can produce varying quantities of DOC (and also Hgtot and MeHg) stream concentrations (Figure 15).

St. Louis et al. (1994) found that wetlands were the source of the majority of MeHg found in Canadian boreal forest environments. A change in flow regime to a scenario when a greater proportion of precipitation is delivered as rain could facilitate the expansion of wetland areas and thus lead to an increasing trend of MeHg production and stream water concentration.

5.2 Model performance

The dynamic versions of RIM, RIM_{dyn} and RIM_{med}, both outperformed RIM_{static}. However the dynamic versions of RIM both had weaknesses. The sine wave used in RIM_{dyn} was generally not flexible enough to model abrupt seasonal changes. The RIM_{med}'s flexibility helped it to outperform RIM_{dyn}, on all but one occasion (based on the metrics used within the study to quantify model performance) (table 4.2) but it was also susceptible to being skewed by months with a median much larger than other months within the year. This is because the monthly values assigned are scaled relative to the median for the entire dataset, extreme values will make months in the rest of the year seem like they are low and the model may overcompensate and increase predicted values for months which RIM_{static} (on which RIM_{med} is based) has already over-predicted. The model makes up for these errors by doing a better job of predicting extreme months, overall there was a net improvement but it should be noted that in situations when trends are extreme but follow a monotonic pattern of increase and decrease, RIM_{dyn} using its sine wave would produce better simulated values.

Previous research using the RIM to model stream water concentrations of DOC also found that dynamics versions of the RIM model outperformed static versions (Oni et al. 2014; Winterdahl, Futter, et al. 2011). Winterdahl, Futter, et al. (2011) and Oni et al. (2014) achieved higher NSEs ranging between 0.42 – 0.58 and 0.52 – 0.62 through the incorporation of soil solution profile data, compared to 0.14 – 0.30 found in this study. Seibert et al. (2009) also used the RIM_{static} model to model stream water TOC at site C2 with RMSEs of 1.4 – 11.6 mg/L which are a similar range to RMSEs for DOC stream water concentration from the RIM_{static} model used in this study 6.7 – 10.5 mg/L.

A study conducted by Gilmour et al. (1998) found that in the Florida Everglades there was a strong correlations between locations of high MeHg production and high MeHg stream water concentration, suggesting that in situ production is the most important factors for MeHg concentrations. This could be a possible explanation for the fluctuations and seemingly non-seasonal patterns observed in the Svartberget catchment. The study in the Everglades also found that MeHg production was inversely correlated to sulphide concentrations, this was supported by experimental findings which found reduced rates of MeHg production when sulphate reducing bacteria were inhibited (Compeau and Bartha 1985; Gilmour, Henry, and Mitchell 1992). This suggests that flow is not the main driver governing MeHg stream water concentrations and explains why RIM predictions for MeHg were not as close to observed values as they were for DOC.

Lee and Iverfeldt (1991) found evidence to suggest that Hg and MeHg were closely associated with organic substances in water. However Hg and MeHg did not follow DOC trends in this study. This could be for a number of reasons. The findings in Lee and Iverfeldt's (1991) study were based on absorbance (water colour); this could be that quality of DOC which has been should to be related to its quality, could be the controlling factor and not just the stream water concentration. Lee and Iverfeldt's (1991) findings were corroborated in a study by St. Louis et al. (1994) conducted in Canada.

5.3 Interaction with other substances within the riparian zone

This study was limited to a relatively few parameters: temperature, flow and solute concentrations for DOC, Hg and MeHg. In practices this solutes are interacting with other substances within the riparian zone and competing with other cations (Monteith et al. 2007; Schroeder, Munthe, and Lindqvist 1989). Also parameters such as pH and redox have been shown to be important determinant for the speciation and mobilisation of solute within the soil system (Gabriel and Williamson 2004).

As the RIM model does not consider these parameters, they could be responsible for creating much of the seemingly unexplained variation in the response between flow and solute stream water concentration.

6. Conclusion and Recommendations

The results in this study were consisting with previous studies which indicate that DOC stream water concentrations are following an upward trend in the decade. The variation in RIM's ability to accurately, or at least consistently (the same model can over or under predict value for the same solute at different sites), simulate stream water concentrations highlights the complexity of the cycling of solutes throughout at catchment also the influence that catchment characteristics play on solute cycling throughout a catchment.

Climate change within the boreal region is having dramatic impacts on catchment dynamics as the hydrology and biochemistry is been altered. With the current trend of increasing average annual temperatures it is likely that the changes within the boreal region will continue to occur and may occur at an enhanced rate in future. A study conducted by Köhler et al. (2009) found that under two different climate conditions based on forecasts by the IPCC for boreal regions, that TOC could potentially be between 1.5 – 2.5 mg/L higher which equates to a 15% increase.

Yurova et al. (2008) found that inter-annual variability in DOC production within a mire was controlled by flow intensity and microbial action (which in turn is controlled by temperature and aeration). A changing climate will impact all of these parameters. Warmer temperatures will allow for increase rates of microbial action, alter freeze-thaw cycles (which improve aeration) and produce a new flow regime (a large proportion of precipitation will be delivered as rain as opposed to snow).

In light of this, it is necessary to develop a better understanding of factors which drive important solutes such as DOC and Hg to be able to inform current and future strategies on a wide range of social and environmental issues. Knowledge regarding DOC and Hg dynamics should be used to guide social decisions on which lakes to open for recreational fishing, where and when to target awareness campaigns and Hg contamination warnings. Habitat protection and restoration will also benefit from being target in areas where they will have the greatest impact.

Winterdahl, Futter, et al. (2011) conducted research into DOC dynamics across Sweden and proposed that catchments can be classified into four classes (flow-driven, seasonal, snowmelt-dominated and nonseasonal) according to observed DOC dynamics. The viability of applying this or a similar classification system to other solutes such as Hg should be investigated as the results could be used to educate decisions on which version of RIM would be most appropriate for a particular catchment/solute combination.

With regards to modelling solute concentrations the RIM model is a very useful tool. Despite its parsimonious data requirements, in many cases it offers reasonable simulations of stream water concentrations. Further research should be conducted into exploring and improving versions of RIM and a catchment and/or month classi-

fication system could be developed specifying which version of RIM is most likely to be offer the most accurate predictions for a specific catchment and/or time period.

7. References

Aastrup, Mats, Jacob Johnson, Ewa Bringmark, Iage Bringmark, and Åke Iverfeldt. 1991. "Occurence and Transport of Mercury within a Small Catchment Area." *Water Air & Soil Pollution* 56 (1): 155–67. doi:10.1007/BF00342269.

Ågren, Anneli, Ishi Buffam, Martin Berggren, Kevin Bishop, Mats Jansson, and Hjalmar Laudon. 2008. "Dissolved Organic Carbon Characteristics in Boreal Streams in a Forest-Wetland Gradient during the Transition between Winter and Summer." *Journal of Geophysical Research: Biogeosciences* 113 (G3): G03031. doi:10.1029/2007JG000674.

Åkerblom, Staffan, Anders Bignert, Markus Meili, Lars Sonesten, and Marcus Sundbom. 2014. "Half a Century of Changing Mercury Levels in Swedish Freshwater Fish." *AMBIO* 43 (1): 91–103. doi:10.1007/s13280-014-0564-1.

Åkerblom, Staffan, Markus Meili, Lage Bringmark, Kjell Johansson, Dan Berggren Kleja, and Bo Bergkvist. 2008. "Partitioning of Hg Between Solid and Dissolved Organic Matter in the Humus Layer of Boreal Forests." *Water, Air, and Soil Pollution* 189 (1-4): 239–52. doi:10.1007/s11270-007-9571-1.

Babiarz, Christopher L., James P. Hurley, David P. Krabbenhoft, Cynthia Gilmour, and Brian A. Branfireun. 2003. "Application of Ultrafiltration and Stable Isotopic Amendments to Field Studies of Mercury Partitioning to Filterable Carbon in Lake Water and Overland Runoff." *Science of The Total Environment*, Pathways and processes of mercury in the environment. Selected papers presented at the sixth International Conference on Mercury as Global Pollutant, Minamata, Japan, Oct. 15-19, 2001, 304 (1–3): 295–303. doi:10.1016/S0048-9697(02)00576-4.

Bank, Michael S., Cynthia S. Loftin, and Robin E. Jung. 2005. "Mercury Bioaccumulation in Northern Two-Lined Salamanders from Streams in the Northeastern United States." *Ecotoxicology* 14 (1-2): 181–91. doi:10.1007/s10646-004-6268-8.

Bárány, Ebba, Ingvar A. Bergdahl, Lars-Eric Bratteby, Thomas Lundh, Gösta Samuelson, Staffan Skerfving, and Agneta Oskarsson. 2003. "Mercury and Selenium in Whole Blood and Serum in Relation to Fish Consumption and Amalgam Fillings in Adolescents." *Journal of Trace Elements in Medicine and Biology* 17 (3): 165–70. doi:10.1016/S0946-672X(03)80021-4.

Bergman, Inger, Kevin Bishop, Qiang Tu, Wolfgang Frech, Staffan Åkerblom, and Mats Nilsson. 2012. "The Influence of Sulphate Deposition on the Seasonal Variation of Peat Pore Water Methyl Hg in a Boreal Mire." *PLoS ONE* 7 (9): e45547. doi:10.1371/journal.pone.0045547.

Bishop, Kevin, Craig Allan, Lage Bringmark, Edenise Garcia, Sofie Hellsten, Lars Högbom, Kjell Johansson, et al. 2009. "The Effects of Forestry on Hg Bioac-

cumulation in Nemoral/Boreal Waters and Recommendations for Good Silvicultural Practice." *AMBIO: A Journal of the Human Environment* 38 (7): 373–80. doi:10.1579/0044-7447-38.7.373.

Bishop, Kevin H., and Ying-Hua Lee. 1997. "Catchments as a Source of Mercury/methylmercury in Boreal Surface Waters." *Metal Ions in Biological Systems* 34: 113–30.

Bishop, Kevin, Jan Seibert, Stephan Köhler, and Hjalmar Laudon. 2004. "Resolving the Double Paradox of Rapidly Mobilized Old Water with Highly Variable Responses in Runoff Chemistry." *Hydrological Processes* 18 (1): 185–89. doi:10.1002/hyp.5209.

Boening, Dean W. 2000. "Ecological Effects, Transport, and Fate of Mercury: A General Review." *Chemosphere* 40 (12): 1335–51. doi:10.1016/S0045-6535(99)00283-0.

Clark, J. M., S. H. Bottrell, C. D. Evans, D. T. Monteith, R. Bartlett, R. Rose, R. J. Newton, and P. J. Chapman. 2010. "The Importance of the Relationship between Scale and Process in Understanding Long-Term DOC Dynamics." *Science of The Total Environment* 408 (13): 2768–75. doi:10.1016/j.scitotenv.2010.02.046.

Clarkson, Thomas W., Laszlo Magos, and Gary J. Myers. 2003. "The Toxicology of Mercury — Current Exposures and Clinical Manifestations." *New England Journal of Medicine* 349 (18): 1731–37. doi:10.1056/NEJMra022471.

Compeau, G. C., and R. Bartha. 1985. "Sulfate-Reducing Bacteria: Principal Methylators of Mercury in Anoxic Estuarine Sediment." *Applied and Environmental Microbiology* 50 (2): 498–502.

Cory, Neil, Hjalmar Laudon, Stephan Köhler, Jan Seibert, and Kevin Bishop. 2007. "Evolution of Soil Solution Aluminum during Transport along a Forested Boreal Hillslope." *Journal of Geophysical Research: Biogeosciences* 112 (G3): G03014. doi:10.1029/2006JG000387.

Demers, Jason D., Charles T. Driscoll, and James B. Shanley. 2010. "Mercury Mobilization and Episodic Stream Acidification during Snowmelt: Role of Hydrologic Flow Paths, Source Areas, and Supply of Dissolved Organic Carbon." *Water Resources Research* 46 (1): W01511. doi:10.1029/2008WR007021.

Dennis, C. A. R., and F. Fehr. 1975. "The Relationship between Mercury Levels in Maternal and Cord Blood." *Science of The Total Environment* 3 (3): 275–77. doi:10.1016/0048-9697(75)90051-0.

Dietz, Rune, Christian Sonne, Niladri Basu, Birgit Braune, Todd O'Hara, Robert J. Letcher, Tony Scheuhammer, et al. 2013. "What Are the Toxicological Effects of Mercury in Arctic Biota?" *Science of The Total Environment* 443 (January): 775–90. doi:10.1016/j.scitotenv.2012.11.046.

Dittman, Jason A., James B. Shanley, Charles T. Driscoll, George R. Aiken, Ann T. Chalmers, Janet E. Towse, and Pranesh Selvendiran. 2010. "Mercury Dynamics in Relation to Dissolved Organic Carbon Concentration and Quality during High Flow Events in Three Northeastern U.S. Streams." *Water Resources Research* 46 (7): W07522. doi:10.1029/2009WR008351.

Eklöf, Karin, Jens Fölster, Lars Sonesten, and Kevin Bishop. 2012. "Spatial and Temporal Variation of THg Concentrations in Run-off Water from 19 Boreal Catch-

ments, 2000–2010." *Environmental Pollution* 164 (May): 102–9. doi:10.1016/j.envpol.2012.01.024.

Eklöf, Karin, Andrea Kraus, Martyn Futter, Jakob Schelker, Markus Meili, Elizabeth W. Boyer, and Kevin Bishop. 2015. "Parsimonious Model for Simulating Total Mercury and Methylmercury in Boreal Streams Based on Riparian Flow Paths and Seasonality." *Environmental Science & Technology*, June, 150625085250006. doi:10.1021/acs.est.5b00852.

Eklöf, Karin, Jakob Schelker, Rasmus Sørensen, Markus Meili, Hjalmar Laudon, Claudia von Brömssen, and Kevin Bishop. 2014. "Impact of Forestry on Total and Methyl-Mercury in Surface Waters: Distinguishing Effects of Logging and Site Preparation." *Environmental Science & Technology* 48 (9): 4690–98. doi:10.1021/es404879p.

Elghany, N. A., W. Stopford, W. B. Bunn, and L. E. Fleming. 1997. "Occupational Exposure to Inorganic Mercury Vapour and Reproductive Outcomes." *Occupational Medicine* 47 (6): 333–36. doi:10.1093/occmed/47.6.333.

European Commission. 2012. "Report on the Implementation of the Water Framework Directive (2000/60/EC)." Brussels: European Commission. http://ec.europa.eu/environment/water/water-framework/pdf/CWD-2012-379_EN-Vol2.pdf.

Fleming, E. J., E. E. Mack, P. G. Green, and D. C. Nelson. 2006. "Mercury Methylation from Unexpected Sources: Molybdate-Inhibited Freshwater Sediments and an Iron-Reducing Bacterium." *Applied and Environmental Microbiology* 72 (1): 457–64. doi:10.1128/AEM.72.1.457-464.2006.

French, Todd D., Adam J. Houben, Jean-Pierre W. Desforges, Linda E. Kimpe, Steven V. Kokelj, Alexandre J. Poulain, John P. Smol, Xiaowa Wang, and Jules M. Blais. 2014. "Dissolved Organic Carbon Thresholds Affect Mercury Bioaccumulation in Arctic Lakes." *Environmental Science & Technology* 48 (6): 3162–68. doi:10.1021/es403849d.

Gabriel, Mark, and Derek Williamson. 2004. "Principal Biogeochemical Factors Affecting the Speciation and Transport of Mercury through the Terrestrial Environment." *Environmental Geochemistry and Health* 26 (February): 412–34.

Gilmour, Cynthia C., Elizabeth A. Henry, and Ralph Mitchell. 1992. "Sulfate Stimulation of Mercury Methylation in Freshwater Sediments." *Environmental Science & Technology* 26 (11): 2281–87.

Gilmour, Cynthia C., G. S. Riedel, M. C. Ederington, J. T. Bell, G. A. Gill, and M. C. Stordal. 1998. "Methylmercury Concentrations and Production Rates across a Trophic Gradient in the Northern Everglades." *Biogeochemistry* 40 (2-3): 327–45. doi:10.1023/A:1005972708616.

Gochfeld, Michael. 2003. "Cases of Mercury Exposure, Bioavailability, and Absorption." *Ecotoxicology and Environmental Safety*, Special Issue on Methodologies for Assessing Exposures to Metals: Speciation, Bioaccessibility and Bioavailability in the Environment, Food and Feed, 56 (1): 174–79. doi:10.1016/S0147-6513(03)00060-5.

Graham, Andrew M., George R. Aiken, and Cynthia C. Gilmour. 2012. "Dissolved Organic Matter Enhances Microbial Mercury Methylation Under Sulfidic Conditions." *Environmental Science & Technology* 46 (5): 2715–23. doi:10.1021/

es203658f.

Hamed, Khaled H., and A. Ramachandra Rao. 1998. "A Modified Mann-Kendall Trend Test for Autocorrelated Data." *Journal of Hydrology* 204 (1–4): 182–96. doi:10.1016/S0022-1694(97)00125-X.

Hintelmann, Holger, Reed Harris, Andrew Heyes, James P. Hurley, Carol A. Kelly, David P. Krabbenhoft, Steve Lindberg, John W. M. Rudd, Karen J. Scott, and Vincent L. St.Louis. 2002. "Reactivity and Mobility of New and Old Mercury Deposition in a Boreal Forest Ecosystem during the First Year of the METAALICUS Study." *Environmental Science & Technology* 36 (23): 5034–40. doi:10.1021/es025572t.

Hoffman, David J., Barnett A. Rattner, G. Allen Burton Jr, and John Cairns Jr. 2002. *Handbook of Ecotoxicology, Second Edition*. CRC Press.

Jackson, Togwell A. 1989. "The Influence of Clay Minerals, Oxides, and Humic Matter on the Methylation and Demethylation of Mercury by Micro-Organisms in Freshwater Sediments." *Applied Organometallic Chemistry* 3 (1): 1–30. doi:10.1002/aoc.590030103.

Johansson, K., B. Bergbäck, and G. Tyler. 2001. "Impact of Atmospheric Long Range Transport of Lead, Mercury and Cadmium on the Swedish Forest Environment." *Water, Air and Soil Pollution: Focus* 1 (3-4): 279–97. doi:10.1023/A:1017528826641.

Johnson, D. W., and S. E. Lindberg. 1995. "The Biogeochemical Cycling of Hg in Forests: Alternative Methods for Quantifying Total Deposition and Soil Emission." *Water, Air, and Soil Pollution* 80 (1-4): 1069–77. doi:10.1007/BF01189767.

Jones, E, P Peterson, and et al. 2014. *SciPy: Open Source Scientific Tools for Python*. Accessed March 26. http://www.scipy.org/.

Köhler, S. J., I. Buffam, H. Laudon, and K. H. Bishop. 2008. "Climate's Control of Intra-Annual and Interannual Variability of Total Organic Carbon Concentration and Flux in Two Contrasting Boreal Landscape Elements." *Journal of Geophysical Research: Biogeosciences* 113 (G3): G03012. doi:10.1029/2007JG000629.

Köhler, S. J., I. Buffam, J. Seibert, K. H. Bishop, and H. Laudon. 2009. "Dynamics of Stream Water TOC Concentrations in a Boreal Headwater Catchment: Controlling Factors and Implications for Climate Scenarios." *Journal of Hydrology* 373 (1–2): 44–56. doi:10.1016/j.jhydrol.2009.04.012.

Kolka, Randall, Peter Weishampel, and Mats Fröberg. 2008. "Measurement and Importance of Dissolved Organic Carbon." In *Field Measurements for Forest Carbon Monitoring*, 171–76. Springer. http://link.springer.com/chapter/10.1007/978-1-4020-8506-2_13.

Korsman, Tom. 1999. "Temporal and Spatial Trends of Lake Acidity in Northern Sweden." *Journal of Paleolimnology* 22 (1): 1–15. doi:10.1023/A:1008003218065.

Kronberg, Rose-Marie. 2014. "The boreal journey of methyl mercury." Doctoral thesis. http://pub.epsilon.slu.se/10994/.

Langston, William J., and Maria J. Bebianno. 1998. *Metal Metabolism in Aquatic Environments*. Springer.

Laudon, Hjalmar, Stephan Köhler, and Kevin H Bishop. 1999. "Natural Acidity or Anthropogenic Acidification in the Spring Flood of Northern Sweden?" *Science*

of The Total Environment 234 (1–3): 63–73. doi:10.1016/S0048-9697(99)00259-4.

Lee, Y. H., K. Bishop, C. Pettersson, ÅIverfeldt, and B. Allard. 1995. "Subcatchment Output of Mercury and Methylmercury at Svartberget in Northern Sweden." *Water, Air, and Soil Pollution* 80 (1-4): 455–65.

Lee, Ying-Hua, and Åke Iverfeldt. 1991. "Measurement of Methylmercury and Mercury in Run-Off, Lake and Rain Waters." *Water Air & Soil Pollution* 56 (1): 309–21. doi:10.1007/BF00342279.

Lewerenz, H.-J. 1991. "Methylmercury (Environmental Health Criteria No. 101). 144 Seiten, 5 Abb. 11 Tab. World Health Organization, Geneva 1990. Preis: 16, — Sw.fr.; 12,80 US $." *Food / Nahrung* 35 (3): 326–27. doi:10.1002/food.19910350318.

Lindqvist, Oliver, Kjell Johansson, Lage Bringmark, Birgitta Timm, Mats Aastrup, Arne Andersson, Gunnar Hovsenius, Lars Håkanson, Åke Iverfeldt, and Markus Meili. 1991. "Mercury in the Swedish Environment — Recent Research on Causes, Consequences and Corrective Methods." *Water, Air, and Soil Pollution* 55 (1-2): xi – 261. doi:10.1007/BF00542429.

MacGregor, J. T., and T. W. Clarkson. 1974. "Distribution, Tissue Binding and Toxicity of Mercurials." In *Protein-Metal Interactions*, edited by Mendel Friedman, 463–503. Advances in Experimental Medicine and Biology 48. Springer New York. http://link.springer.com/chapter/10.1007/978-1-4684-0943-7_22.

Mierle, G., and R. Ingram. 1991. "The Role of Humic Substances in the Mobilization of Mercury from Watersheds." *Water Air & Soil Pollution* 56 (1): 349–57. doi:10.1007/BF00342282.

Monteith, Donald T., John L. Stoddard, Christopher D. Evans, Heleen A. de Wit, Martin Forsius, Tore Høgåsen, Anders Wilander, et al. 2007. "Dissolved Organic Carbon Trends Resulting from Changes in Atmospheric Deposition Chemistry." *Nature* 450 (7169): 537–40. doi:10.1038/nature06316.

Moré, Jorge J. 1978. "The Levenberg-Marquardt Algorithm: Implementation and Theory." In *Numerical Analysis*, 105–16. Springer Berlin Heidelberg. http://link.springer.com/content/pdf/10.1007/BFb0067700.pdf.

Munthe, John, Sofie Hellsten, and Therese Zetterberg. 2007. "Mobilization of Mercury and Methylmercury from Forest Soils after a Severe Storm-Fell Event." *AMBIO: A Journal of the Human Environment* 36 (1): 111–13. doi:10.1579/0044-7447(2007)36[111:MOMAMF]2.0.CO;2.

Munthe, John, and Hans Hultberg. 2004. "Mercury and Methylmercury in Runoff from a Forested Catchment – Concentrations, Fluxes, and Their Response to Manipulations." *Water, Air and Soil Pollution: Focus* 4 (2-3): 607–18. doi:10.1023/B:WAFO.0000028381.04393.ed.

Munthe, John, Hans Hultberg, and Åke Iverfeldt. 1995. "Mechanisms of Deposition of Methylmercury and Mercury to Coniferous Forests." In *Mercury as a Global Pollutant*, edited by Donald B. Porcella, John W. Huckabee, and Brian Wheatley, 363–71. Springer Netherlands. http://link.springer.com/chapter/10.1007/978-94-011-0153-0_40.

Nagelkerke, N. J. D. 1991. "A Note on a General Definition of the Coefficient of Determination." *Biometrika* 78 (3): 691–92. doi:10.2307/2337038.

Ninomiya, T., H. Ohmori, K. Hashimoto, K. Tsuruta, and S. Ekino. 1995. "Expansion of Methylmercury Poisoning Outside of Minamata: An Epidemiological Study on Chronic Methylmercury Poisoning outside of Minamata." *Environmental Research* 70 (1): 47–50. doi:10.1006/enrs.1995.1045.

Oni, S. K., M. N. Futter, K. Bishop, S. J. Köhler, M. Ottosson-Löfvenius, and H. Laudon. 2013. "Long-Term Patterns in Dissolved Organic Carbon, Major Elements and Trace Metals in Boreal Headwater Catchments: Trends, Mechanisms and Heterogeneity." *Biogeosciences* 10 (4): 2315–30. doi:10.5194/bg-10-2315-2013.

Oni, S. K., M. N. Futter, Claudia Teutschbein, and Hjalmar Laudon. 2014. "Cross-Scale Ensemble Projections of Dissolved Organic Carbon Dynamics in Boreal Forest Streams." *Climate Dynamics* 42 (9-10): 2305–21. doi:10.1007/s00382-014-2124-6.

Patra, Manomita, and Archana Sharma. 2000. "Mercury Toxicity in Plants." *The Botanical Review* 66 (3): 379–422. doi:10.1007/BF02868923.

Porvari, Petri, Matti Verta, John Munthe, and Merja Haapanen. 2003. "Forestry Practices Increase Mercury and Methyl Mercury Output from Boreal Forest Catchments." *Environmental Science & Technology* 37 (11): 2389–93. doi:10.1021/es0340174.

Ravichandran, Mahalingam. 2004. "Interactions between Mercury and Dissolved Organic Matter—a Review." *Chemosphere* 55 (3): 319–31. doi:10.1016/j.chemosphere.2003.11.011.

Ravichandran, Mahalingam, George R. Aiken, Joseph N. Ryan, and Michael M. Reddy. 1999. "Inhibition of Precipitation and Aggregation of Metacinnabar (Mercuric Sulfide) by Dissolved Organic Matter Isolated from the Florida Everglades." *Environmental Science & Technology* 33 (9): 1418–23. doi:10.1021/es9811187.

Reimers, Robert S., and Peter A. Krenkel. 1974. "Kinetics of Mercury Adsorption and Desorption in Sediments." *Journal (Water Pollution Control Federation)* 46 (2): 352–65.

Sarkkola, Sakari, Harri Koivusalo, Ari Laurén, Pirkko Kortelainen, Tuija Mattsson, Marjo Palviainen, Sirpa Piirainen, Mike Starr, and Leena Finér. 2009. "Trends in Hydrometeorological Conditions and Stream Water Organic Carbon in Boreal Forested Catchments." *Science of The Total Environment* 408 (1): 92–101. doi:10.1016/j.scitotenv.2009.09.008.

Schaefli, Bettina, and Hoshin V. Gupta. 2007. "Do Nash Values Have Value?" *Hydrological Processes* 21 (15): 2075–80. doi:10.1002/hyp.6825.

Schroeder, W.H., J. Munthe, and O. Lindqvist. 1989. "Cycling of Mercury between Water, Air, and Soil Compartments of the Environment." *Water, Air, and Soil Pollution* 48 (April): 337–47.

Schuster, E. 1991. "The Behavior of Mercury in the Soil with Special Emphasis on Complexation and Adsorption Processes - A Review of the Literature." *Water Air & Soil Pollution* 56 (1): 667–80. doi:10.1007/BF00342308.

Seibert, J., T. Grabs, S. Köhler, H. Laudon, M. Winterdahl, and K. Bishop. 2009. "Linking Soil- and Stream-Water Chemistry Based on a Riparian Flow-Concentration Integration Model." *Hydrol. Earth Syst. Sci.* 13 (12): 2287–97. doi:10.5194/hess-13-2287-2009.

Selin, Noelle E. 2009. "Global Biogeochemical Cycling of Mercury: A Review."

Annual Review of Environment and Resources 34 (1): 43–63. doi:10.1146/annurev.environ.051308.084314.

Skogsstyrelsen [Swedish Forest Agency]. 2014. "Skogsstyrelsen [Swedish Forest Agency]." *Swedish Forest Agency: Economy Statistics*. June. http://www.skogsstyrelsen.se/en/AUTHORITY/Statistics/Subject-Areas/Economy/Economy/.

Skyllberg, Ulf. 2008. "Competition among Thiols and Inorganic Sulfides and Polysulfides for Hg and MeHg in Wetland Soils and Sediments under Suboxic Conditions: Illumination of Controversies and Implications for MeHg Net Production." *Journal of Geophysical Research: Biogeosciences* 113 (G2): G00C03. doi:10.1029/2008JG000745.

Sørensen, Rasmus, Markus Meili, Lars Lambertsson, Claudia von Brömssen, and Kevin Bishop. 2009. "The Effects of Forest Harvest Operations on Mercury and Methylmercury in Two Boreal Streams: Relatively Small Changes in the First Two Years prior to Site Preparation." *AMBIO: A Journal of the Human Environment* 38 (7): 364–72. doi:10.1579/0044-7447-38.7.364.

St. Louis, Vincent L., John W. M. Rudd, Carol A. Kelly, Ken G. Beaty, Nicholas S. Bloom, and Robert J. Flett. 1994. "Importance of Wetlands as Sources of Methyl Mercury to Boreal Forest Ecosystems." *Canadian Journal of Fisheries and Aquatic Sciences* 51 (5): 1065–76. doi:10.1139/f94-106.

Trasande, Leonardo, Philip J. Landrigan, and Clyde Schechter. 2005. "Public Health and Economic Consequences of Methyl Mercury Toxicity to the Developing Brain." *Environmental Health Perspectives* 113 (5): 590–96.

Travnikov, O. 2005. "Contribution of the Intercontinental Atmospheric Transport to Mercury Pollution in the Northern Hemisphere." *Atmospheric Environment* 39 (39): 7541–48. doi:10.1016/j.atmosenv.2005.07.066.

Ullrich, Susanne M., Trevor W. Tanton, and Svetlana A. Abdrashitova. 2001. "Mercury in the Aquatic Environment: A Review of Factors Affecting Methylation." *Critical Reviews in Environmental Science and Technology* 31 (3): 241–93. doi:10.1080/20016491089226.

United Nations Environmental Programme, Chemicals. 2002. "Global Mercury Assessment." Geneva, Switzerland: United Nations Environmental Programme (UNEP) Chemicals.

Wallach, D., and B. Goffinet. 1989. "Mean Squared Error of Prediction as a Criterion for Evaluating and Comparing System Models." *Ecological Modelling* 44 (3–4): 299–306. doi:10.1016/0304-3800(89)90035-5.

Wang, Feiyue, and JinZhong Zhang. 2012. "Mercury Contamination in Aquatic Ecosystems under a Changing Environment: Implications for the Three Gorges Reservoir." *Chinese Science Bulletin* 58 (2): 141–49. doi:10.1007/s11434-012-5490-7.

Wennberg, Maria, Thomas Lundh, Ingvar A. Bergdahl, Göran Hallmans, Jan-Håkan Jansson, Birgitta Stegmayr, Hipolito M. Custodio, and Staffan Skerfving. 2006. "Time Trends in Burdens of Cadmium, Lead, and Mercury in the Population of Northern Sweden." *Environmental Research* 100 (3): 330–38. doi:10.1016/j.envres.2005.08.013.

Winterdahl, Mattias, Martin Erlandsson, Martyn N. Futter, Gesa A. Weyhenmeyer, and Kevin Bishop. 2014. "Intra-Annual Variability of Organic Carbon Concentrations in Running Waters: Drivers along a Climatic Gradient." *Global Biogeochemical Cycles* 28 (4): 2013GB004770. doi:10.1002/2013GB004770.

Winterdahl, Mattias, Martyn Futter, Stephan Köhler, Hjalmar Laudon, Jan Seibert, and Kevin Bishop. 2011. "Riparian Soil Temperature Modification of the Relationship between Flow and Dissolved Organic Carbon Concentration in a Boreal Stream: MODELING STREAM DISSOLVED ORGANIC CARBON." *Water Resources Research* 47 (8): n/a – n/a. doi:10.1029/2010WR010235.

Winterdahl, Mattias, Johan Temnerud, Martyn N. Futter, Stefan Löfgren, Filip Moldan, and Kevin Bishop. 2011. "Riparian Zone Influence on Stream Water Dissolved Organic Carbon Concentrations at the Swedish Integrated Monitoring Sites." *AMBIO* 40 (8): 920–30. doi:10.1007/s13280-011-0199-4.

YANG, Yong-kui, Cheng ZHANG, Xiao-jun SHI, Tao LIN, and Ding-yong WANG. 2007. "Effect of Organic Matter and pH on Mercury Release from Soils." *Journal of Environmental Sciences* 19 (11): 1349–54. doi:10.1016/S1001-0742(07)60220-4.

Yurova, Alla, Andrey Sirin, Ishi Buffam, Kevin Bishop, and Hjalmar Laudon. 2008. "Modeling the Dissolved Organic Carbon Output from a Boreal Mire Using the Convection-Dispersion Equation: Importance of Representing Sorption." *Water Resources Research* 44 (7): W07411. doi:10.1029/2007WR006523.

Zahir, Farhana, Shamim J. Rizwi, Soghra K. Haq, and Rizwan H. Khan. 2005. "Low Dose Mercury Toxicity and Human Health." *Environmental Toxicology and Pharmacology* 20 (2): 351–60. doi:10.1016/j.etap.2005.03.007.

Zillioux, E.j., D.b. Porcella, and J.m. Benoit. 1993. "Mercury Cycling and Effects in Freshwater Wetland Ecosystems." *Environmental Toxicology and Chemistry* 12 (12): 2245–64. doi:10.1002/etc.5620121208.

A. Appendix

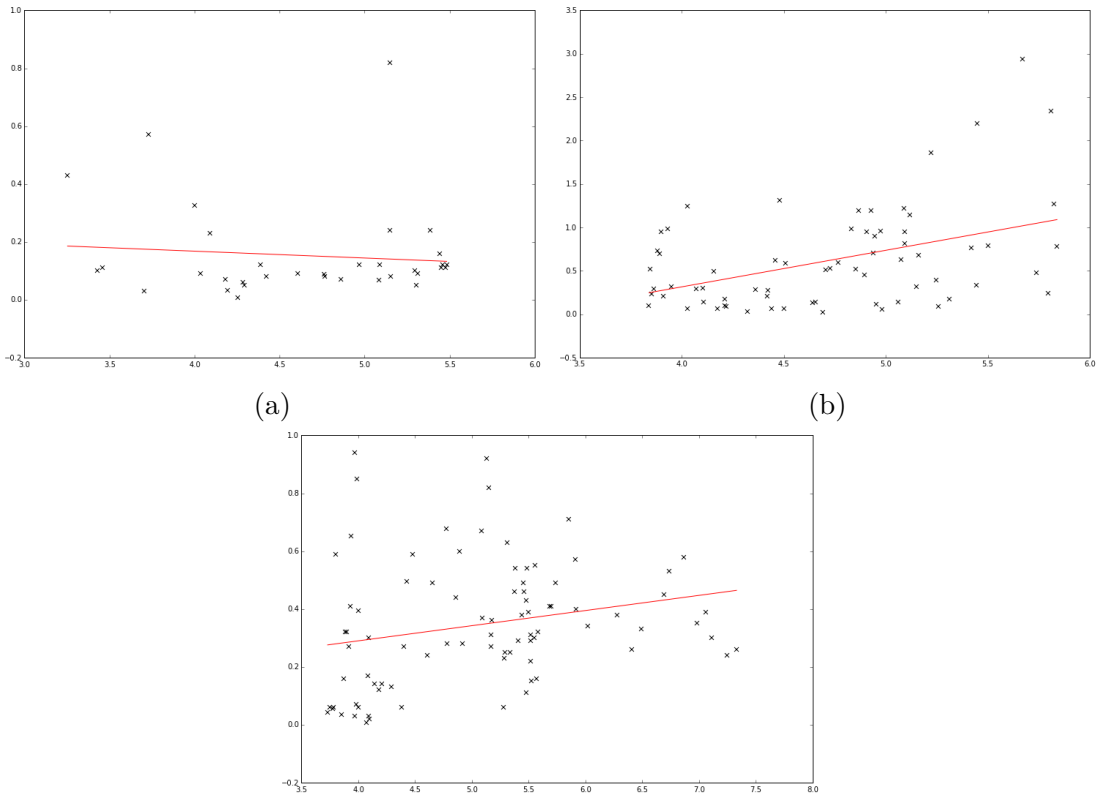

(a) (b) (c)

Figure A.1: Scatter plots of stream water MeHg concentration (ng/L) against average soil temperature (°C) over preceding 30 days at sites C2 (a), C4 (b) and C7 (c).

	Site	R^2	P
DOC mg/L	C2	0.220	<0.001
	C4	0.211	<0.001
	C7	0.075	0.148
Hgtot ng/L	C2	-	-
	C4	-0.018	0.889
	C7	-0.076	0.517
MeHg ng/L	C2	-0.097	0.585
	C4	0.426	<0.001
	C7	0.233	0.031

Table A.1: R^2 coefficients and P-values for linear regression between rolling average 30 day temperature and stream water solute concentration.

	Site	R^2	P
DOC mg/L	C2	0.057	**<0.0001**
	C4	0.124	**<0.0001**
	C7	0.019	**0.004**
Hg_{tot} ng/L	C2	-	-
	C4	0.019	0.192
	C7	0.024	0.113
MeHg ng/L	C2	*0.030*	0.172
	C4	*0.101*	**0.002**
	C7	*0.068*	**0.005**

Table A.2: R^2 and P-values for GWT depth (cm) against solute concentration. Italic values indicate a negative relationship and bold value indicate a statistically significant P-value. α was set at 0.05.

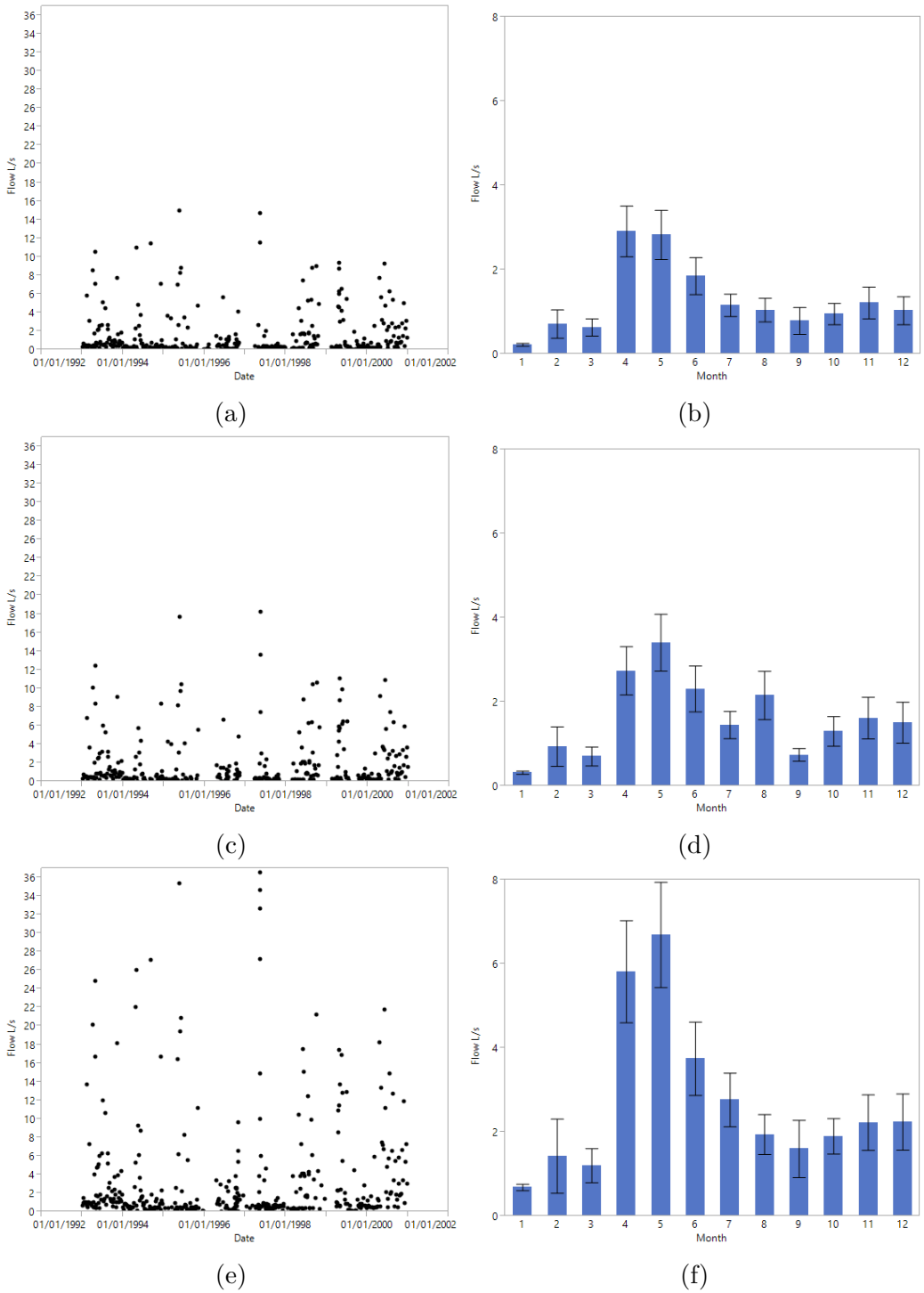

Figure A.2: (Left) flow L/s for sites C2 (a), C4 (c) and C7 (e) and mean monthly flow L/s (right) with error bars for sites C2 (b), C4 (d) and C7 (e) over study period.

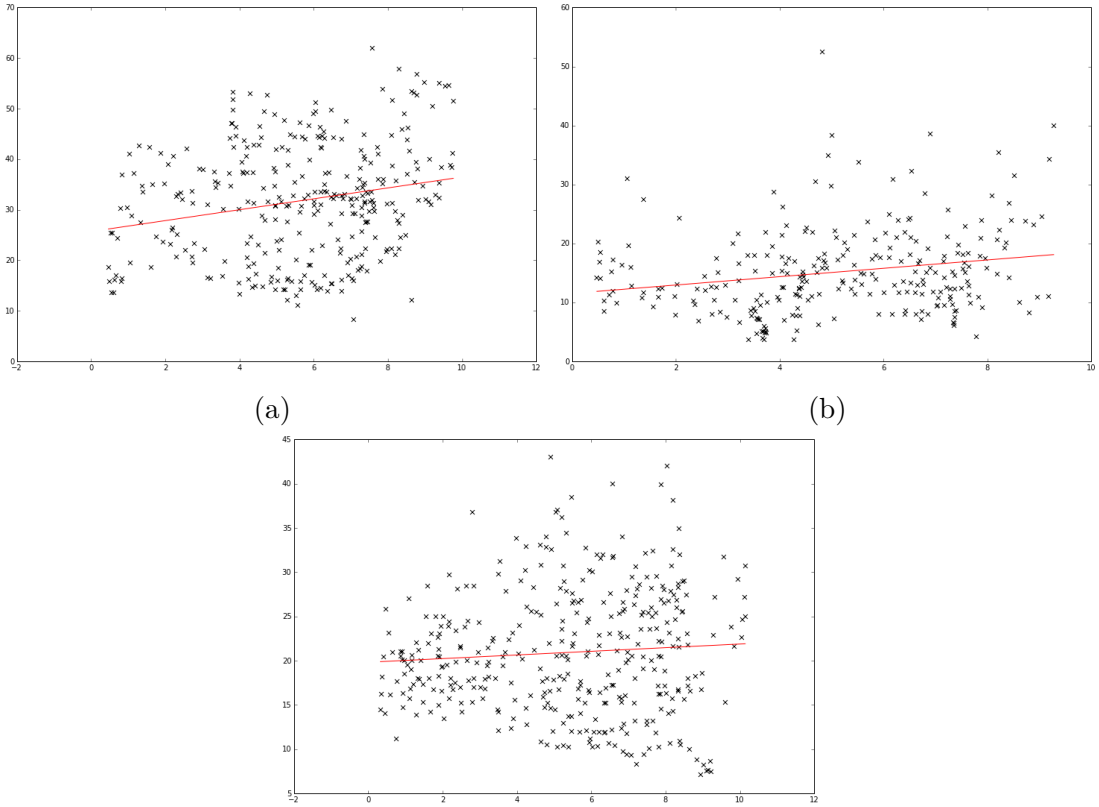

(a) (b)

(c)

Figure A.3: Scatter plots of stream water DOC concentration (mg/L) against average soil temperature (°C) over preceding 30 days at sites C2 (a), C4 (b) and C7 (c).

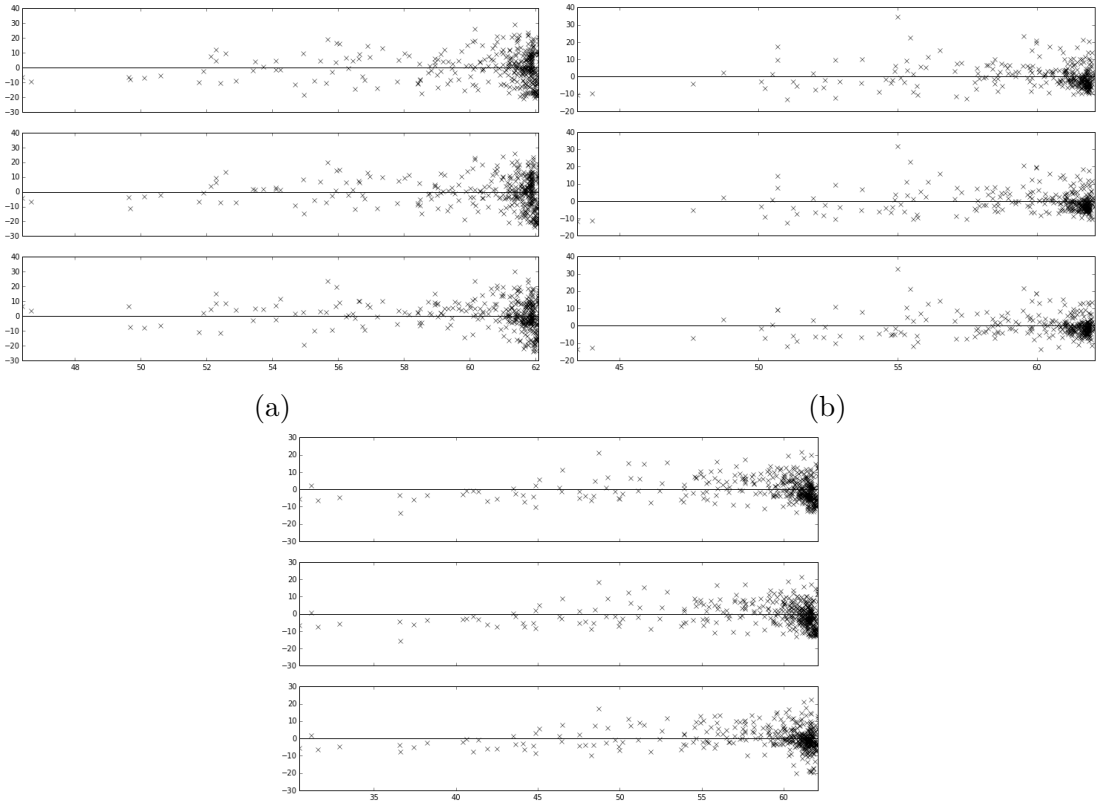

(a) (b)

(c)

Figure A.4: DOC model residuals against depth to groundwater table (cm) for RIM_{static} (top), RIM_{dyn} (middle) and RIM_{med} (bottom) at sites C2 (a), C4 (b) and C7 (c).

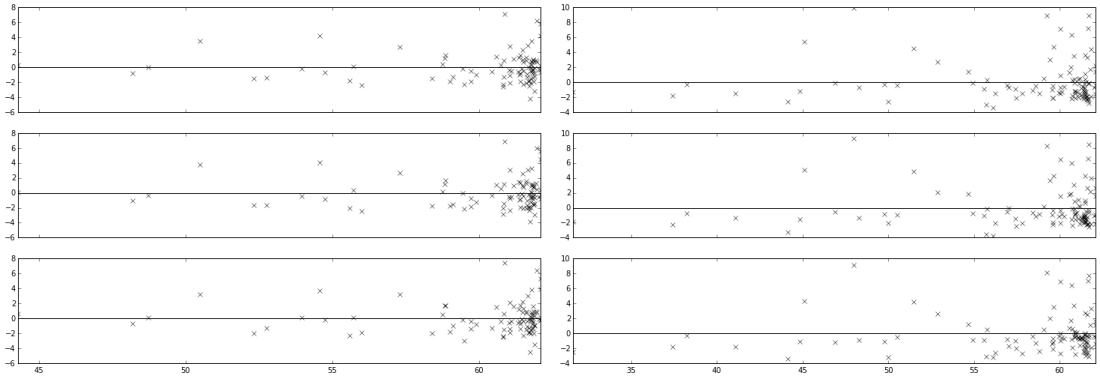

(a) (b)

Figure A.5: Hg_{tot} model residuals against depth to groundwater table (cm) for RIM_{static} (top), RIM_{dyn} (middle) and RIM_{med} (bottom) at sites C4 (a) and C7 (b).

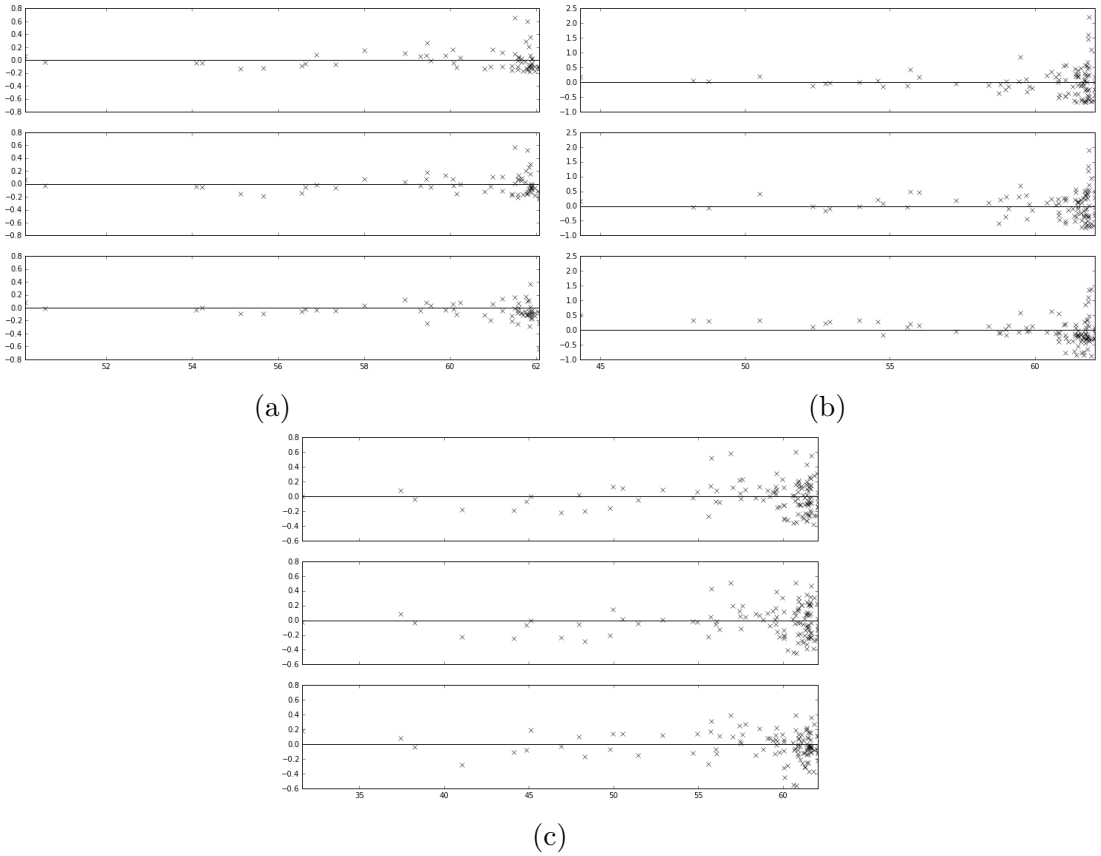

Figure A.6: MeHg model residuals against depth to groundwater table (cm) for RIM_{static} (top), RIM_{dyn} (middle) and RIM_{med} (bottom) at sites C2 (a), C4 (b) and C7 (c).